2014

Manufacturing Techniques Developed for the JetStreamer Dynamic Soaring UAV

Jacob Bruce Patterson
Lehigh University

Manufacturing Techniques Developed for the JetStreamer Dynamic Soaring UAV

by

Jacob Bruce Patterson

A Thesis

Presented to the Graduate and Research Committee

of Lehigh University

in Candidacy for the Degree of

Master of Science

in

Mechanical Engineering

Lehigh University

January 2014

This thesis is accepted and approved in partial fulfillment of the requirements for the Master of Science.

_____

Date

_____

Joachim L. Grenestedt, Advisor

_____

D. Gary Harlow, Chairperson

Department of Mechanical Engineering and Mechanics

Acknowledgements

I would like to thank Dr. Joachim Grenestedt for giving me the opportunity to pursue this project for a Master's thesis. With his guidance I have greatly grown as an engineer as well as developed the skills needed to undertake this project and any one in the future.

I would also like to thank Bill Maroun for his consistent help and input throughout the project. Thank you as well to Rob Thodal and Tianyi Luo for their help in the construction of the wing and their input that consistently improved the process.

Also thank you to Herman Baader who was critical in allowing me to develop my skills as a machinist, which has become invaluable to me in what I do now and what I hope to do in the future.

Finally, thank you to my family for their consistent support throughout my education and for instilling a strong work ethic in me that has been crucial in getting me to where I am today.

Contents

List of Tables

Table of Figures

Abstract

While many theories on dynamic soaring are emerging, most testing of these theories has been done using small R/C aircraft and some basic manned flights. This work focuses on developing and manufacturing the JetStreamer, a 6.5 meter wingspan UAV, to act as a test platform for dynamics soaring techniques. The aircraft's main purpose is to test if dynamic soaring can be done in the jet stream along with real-time wind field estimation.

First, a basic design and analysis was performed for the JetStreamer, from there, small test sections of aircraft components were created to investigate one-shot manufacturing techniques to be used on the full-scale parts. Processes for creating integrated wing spars as well as internal shear webs in a one shot process were developed.

Construction of the JetStreamer then began and during its construction, the one-shot processes were verified on a 6 meter carbon fiber wing. Most notably, the main wing was successfully manufactured using a one-shot process that produced a complete wing with integrated wing spars, an internal shear web structure, and provisions for attachment of control surfaces.

1 Background

Dynamic soaring is a method in which flight is sustained using horizontal wind that varies in strength or direction. Lord Rayleigh was first credited with describing this technique being used by birds in 1883. Seabirds such as the albatross are able to use dynamic soaring techniques to travel hundreds of kilometers in a single day with minimal effort [1]. Recently techniques have been developed that would allow dynamic soaring to be done in the jet stream where there are sufficient wind gradients to support flight of a large airplane. With funding from the National Science Foundation, Lehigh University's Composites Lab is tasked with designing and building an airplane to serve as a test platform to verify these techniques.

From calculations by Prof. Joachim Grenestedt [2], some key parameters that support dynamics soaring are:

- High Lift to Drag ratio
- Ability to perform high g turns
- Energy extraction increases with speed
- High weight in order to increase the terminal velocity and therefore allows the aircraft to operate over a larger vertical range
- Minimal parasitic drag in order to minimize energy loss

1.1 Basic Aircraft Requirements

From the key parameters listed above a few aircraft characteristics are easily identifiable. To maximize the lift to drag ratio, a high wing aspect ratio is desired since it reduces

induced drag. The ability to perform high g load turns is a structural requirement of the aircraft and therefore to maximize g loading the construction materials chosen should be of high strength. Carbon fiber gives a very high specific strength and will be used wherever possible.

One of the less intuitive aircraft parameters is higher weight, but just adding weight to the aircraft creates larger structural requirements. To do this effectively, the weight should be distributed along the wing in order to avoid creating unnecessary bending moments in the wing. So, for the purposes of the dynamic soaring the aircraft should have a high weight with a high aspect ratio wing. Even though high weight is desired, a light aircraft structure should be created since it allows for ballast to be placed in the wings where it does not cause extra structural loadings.

With these basic parameters in mind an initial aircraft concept was generated. The aircraft the Lab is to building will be called the JetStreamer and a concept rendering is shown in figure 1.

Figure 1: JetStreamer Concept Rendering (by Fred Thodal)

The purpose of this thesis is to give an overview of the basic design, performance and construction of the JetStreamer aircraft. Once built it will undergo flight testing and be fitted with a highly capable autopilot to execute the dynamic soaring trajectories. If successful flights are performed at low altitudes the aircraft will then be taken up to the jet stream to begin evaluation of the dynamic soaring routines developed for the jet stream.

1.2 Key Aircraft Design Specifications

While the key design parameters have been identified, a concise design must now be created using this information. To begin, an operating envelope must be determined and for the purpose this project, a maximum speed set at 135 m/s with a 20 g load case (14 g with a 1.4 factor of safety). These specifications offered the performance required during

the dynamic soaring routine to maintain flight in the jet stream. A mass goal of the airframe was then set to be 50kg ready to fly (not including ballast).

Combining the high g load and stiffness requirement with the low weight structure requirement, the construction materials should have a high specific strength and stiffness. One of the best material choices for this is carbon fiber composites.

While the JetStreamer is suppose to have a high aspect ratio wing, compromises must be made to account for structural limitations as well as for the aircraft's dynamic characteristics. Since the aircraft must execute high speed maneuvers, the large polar moment of inertia associated with high aspect ratio wings would impede this. Making some simple structural assumptions for a wing, an aspect ratio of about 20 was decided on. While the wing now has an aspect ratio, actual size must still be determined. At this point the Lab's capabilities were looked over and it was decided that the Lab could produce up to a 6 meter wing in house, but the addition of winglets can further increase the wingspan. To begin, a 6 meter wingspan will be used along with the specified aspect ratio to give a mean chord of 300mm, which in turn gives a wing planform area of 1.8 m^2. Finally a wing shape must be determined. As a compromise between ease of manufacturing and planform efficiency, a linearly tapered wing with a taper ratio of 0.5 was decided on. This gives a root chord of 375mm and a tip chord of 225mm. Additionally, 250mm winglets will be added on the wing tips to further increase the span and aspect ratio.

A summary of the key aircraft design specifications are:

- 135 m/s maximum airspeed

- 20 g maximum load factor
- 50kg ready to fly weight (not including ballast)
- Carbon fiber composite construction
- 6 meter wingspan with 250mm winglets
- 375mm root chord and 204mm tip chord

2 Initial Aerodynamic Analysis

Given these initial design specifications, some basic estimations of the performance of the aircraft can be made and can bring any potential issues to light. To begin, basic data for the chosen airfoil must be obtained to allow us to make reasonable calculations in regards to aircraft performance.

2.1 Airfoil Data

For the sake of time, XFLR5 will be used to generate the airfoil data which will be used for the aircraft performance calculations. XFLR5 is an open-source windows implementation of XFoil algorithm used for the analysis of subsonic airfoils. The airfoil that the JetStreamer will use is a custom profile developed the late Mr. Sven-Olof with some modifications by Prof. Joachim Grenestedt of Lehigh University. The profile shape is shown in the following figure 2 with the coordinates listed in Appendix A.

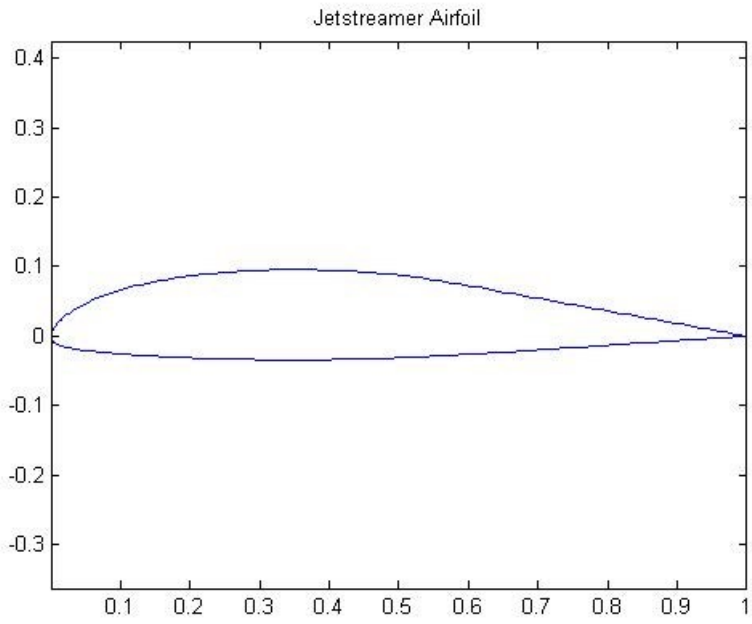

Figure 2: JetStreamer Airfoil Profile

The airfoil shape is then put into XFLR5 to generate the drag polar data as well as other useful design information. Since the airplane will be operating over a large airspeed range there will be a large range of Reynolds numbers. For calculating Reynolds numbers the wing's Mean Aerodynamic Chord (MAC) of 292 mm will be used as the characteristic length of the body. Additionally since the aircraft will initially be tested at low altitude standard sea level conditions will be used for atmospheric properties where T = 15 °C, ρ = 1.23 kg/m³, P = 101.3 kPa, and $\mu = 1.82 * 10^{-6}$ Pa*s.

For the following analysis, it will be assumed the aircraft is operating below Mach 0.3 and therefore flow over the wing will be incompressible. This should be a reasonable assumption since the maximum design speed is Mach 0.4 but the aircraft will be operating below Mach 0.3 for a substantial amount of time, especially during initial testing.

The aircraft will be operating at velocities ranging from 20 m/s to 100 m/s which roughly correspond to Reynolds numbers between 400,000 and 2,000,000 for sea-level conditons. XFLR5 can give airfoil data for given Reynolds numbers and therefore the airfoil characteristics can be determined throughout the range of flight speeds. The following table shows the different flight conditions for which airfoil data was calculated.

Condition #	Re	V(m/s)	M
1	400,000	20	0.06
2	500,000	25	0.07
3	600,000	30	0.09
4	1,000,000	51	0.15
5	1,400,000	71	0.21
6	1,800,000	91	0.27
7	2,000,000	101	0.29

Table 1 :XFLR5 Simulation Paramerters

The Reynolds number and Mach number were put into XFLR5 to perform a steady state analysis on the airfoil. Figures 3 through 6 show some of the simulated characteristics.

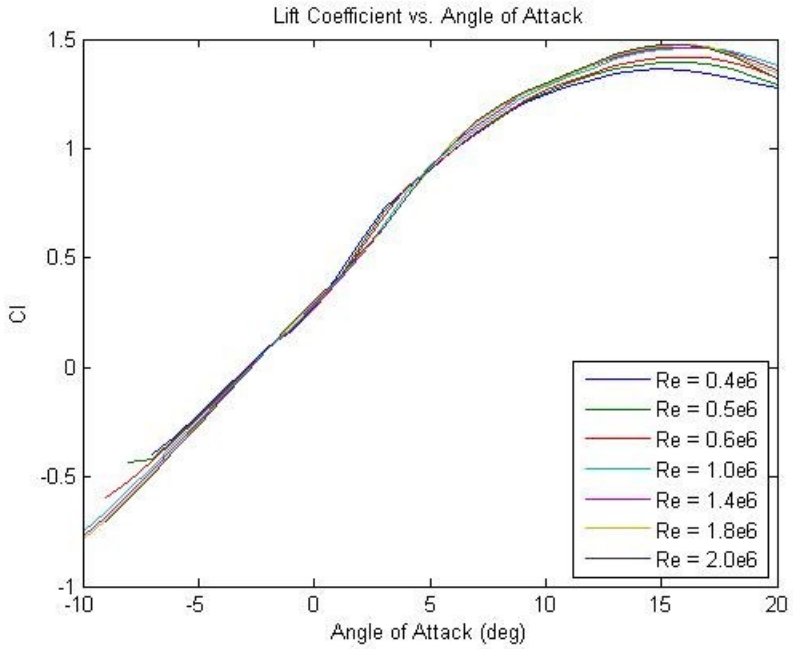

Figure 3: Lift Coefficient vs. Angle of Attack

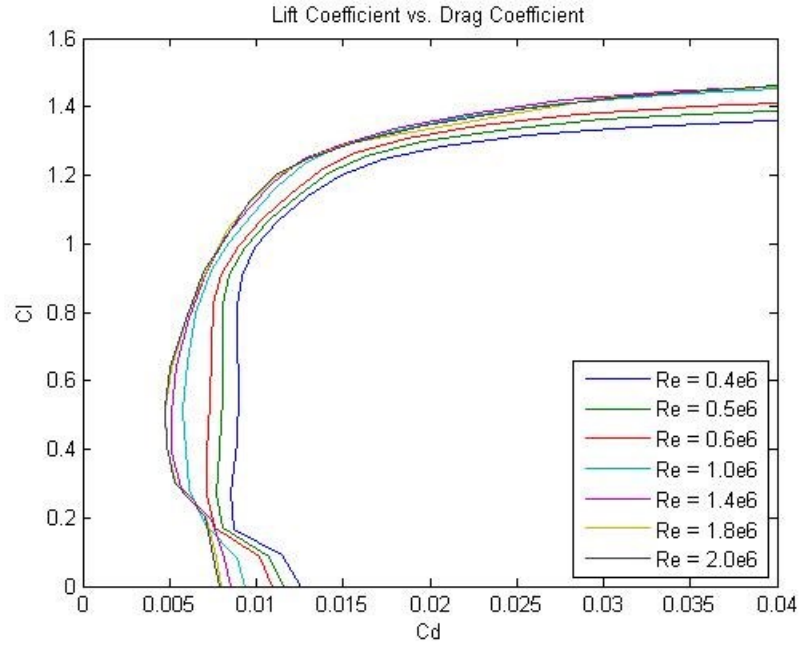

Figure 4: Lift Coefficient vs. Drag Coefficient

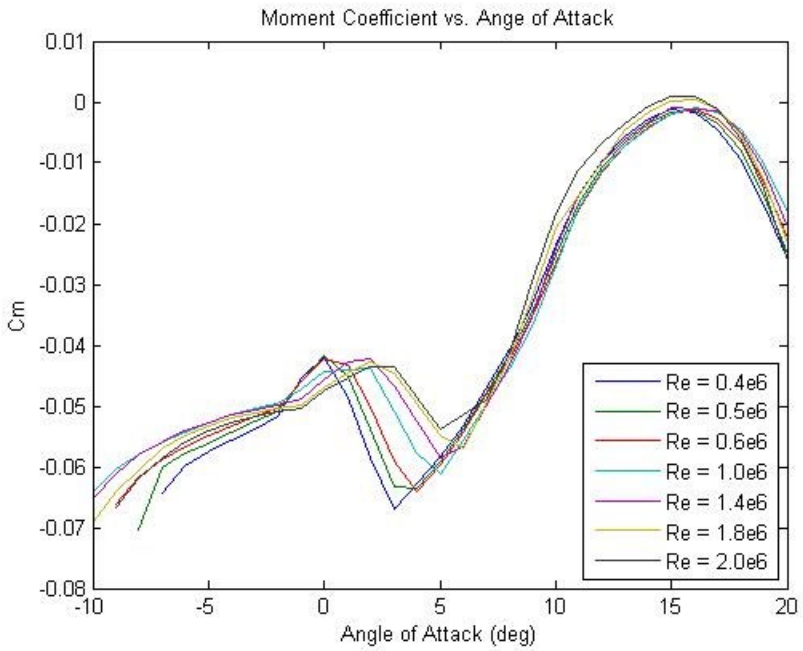

Figure 5: Moment Coefficient vs. Angle of Attack

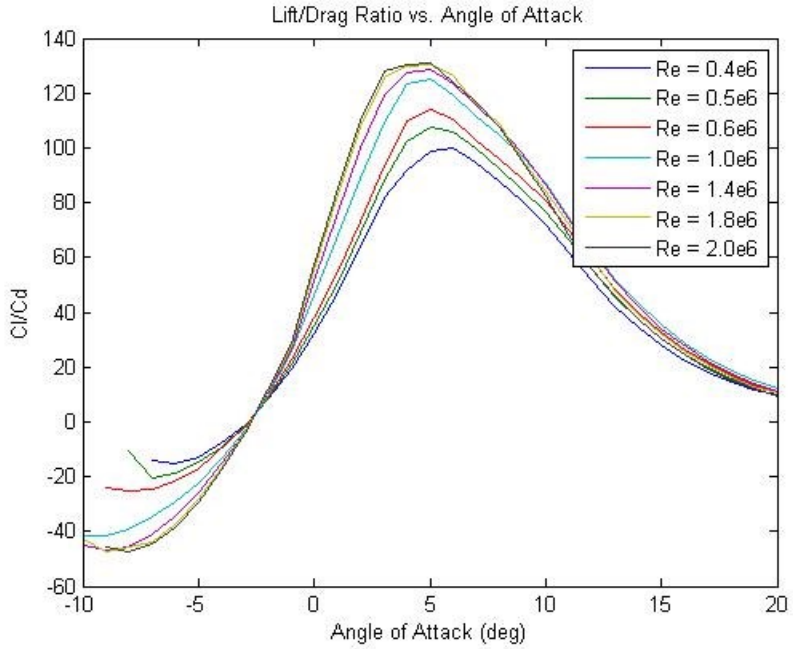

Figure 6: Lift/Drag Ratio vs. Angle of Attack

From these simulations some of the key values of the airfoil can be determined. The main parameter that will be useful is the maximum coefficient of lift which is about 1.3 at the lower Reynolds numbers and up to 1.5 for the higher ones. Additionally, the airfoil has a fairly large drag bucket which is useful for dynamic soaring since during the high g turns the coefficient of lift can be rather high but the airfoil will still keep a rather low form drag coefficient.

The airfoil also has a fairly low moment coefficient for normal flight which will help with wing stability, but this will change dramatically with flaps deployed.

2.2 Lift and Drag Estimations

With this information, a preliminary analysis of the aircraft's performance can be performed. To begin, the plane will be in straight and level flight and therefore lift (L) will be equal to the weight (W) of the plane. Given the initial design mass of the plane, the required lift force can be computed:

$$L = W = m * g = 50 * 9.81 \approx 490\ N \tag{1}$$

Now the required coefficient of lift can be determined for any speed of the aircraft using the following equation:

$$C_l = \frac{L}{\left(\frac{1}{2}\rho V_\infty^2\right) S} \tag{2}$$

with S being the planform area of the aircraft and V_∞ being the airspeed of the aircraft. Rearranging this equation allows for the minimum velocity for the aircraft to be solved for if the maximum value of the coefficient of lift is known. From the simulation a

maximum coefficient of lift will be approximated as 1.3. Using this value, the stall velocity is:

$$V_{Stall} = \sqrt{\frac{2L}{C_{l,max}\,\rho\,S}} = \sqrt{\frac{2 * 490}{1.3 * 1.23 * 1.82}} = 18.4\ m/s \tag{3}$$

This speed is very close to that of the airfoil simulation run at a Reynolds number of 400,000 and therefore, the previous approximations should be relatively close to reality. Using both the coefficient of lift equation and load factor, a V-n diagram can be constructed to help visualize the operating envelope of the plane. XLFR5 had some difficulty computing coefficients for high negative angle of attack and therefore it will be assumed that the airfoil has a maximum negative lift coefficient of -1.0. Using this information the following V-n diagram was constructed.

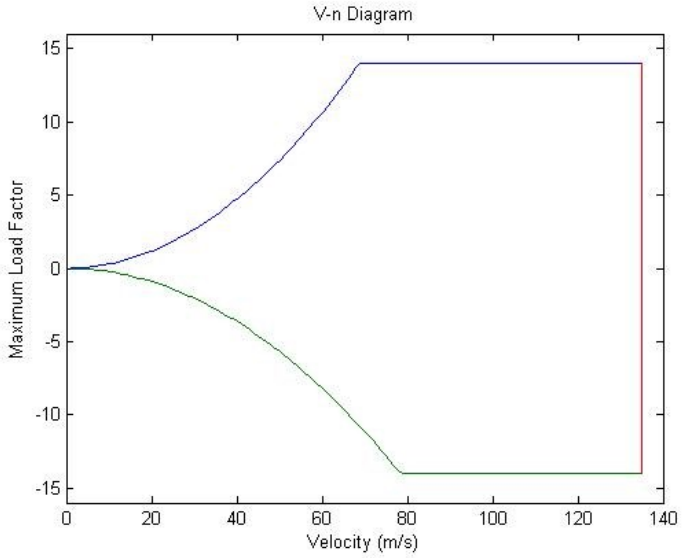

Figure 7: V-n Diagram

Now that the coefficient of lift is a known quantity, the drag of an aircraft can be approximated as:

$$D = C_{d,0_{fuselage}} * A_0 \left(\frac{1}{2}\rho V_\infty^2\right) + C_{d,0_{Airfoil}} * S\left(\frac{1}{2}\rho V_\infty^2\right) + C_{d,i} * S\left(\frac{1}{2}\rho V_\infty^2\right) \quad (4)$$

Where $C_{d,0}$ is the zero-lift drag coefficient, $C_{d,i}$ is the induced drag coefficient, and A_0 is the frontal area of the fuselage. The induced drag coefficient can be approximated as:

$$C_{d,i} = \frac{C_l^2}{\pi e \Lambda} \quad (5)$$

Where e is the Oswald efficiency factor, Λ is the wing aspect ratio. Typically for subsonic aircraft the Oswald efficiency factor varies between 0.7 and 0.85 [3]. For a first approximation the Oswald efficiency factor will be assumed to be 0.8, which is fairly consistent with other aircraft of this planform shape. Continuing on, the zero-lift drag coefficient of the wing will be approximated from figure 4 as 0.008. Additionally, the drag coefficient of the fuselage will be accounted for by assuming it is a streamlined body with a drag coefficient of 0.05.

Combining equations 1,2, 4, and 5, the drag of the aircraft can be reduced to a function of velocity only. A MATLAB program was created to determine the drag force for velocities ranging from 10 m/s to 100 m/s and is given in Appendix B. With knowledge of both the lift and drag forces as a function of velocity, a variety of useful plots can be generated. To begin, figure 8 shows drag vs. aircraft velocity.

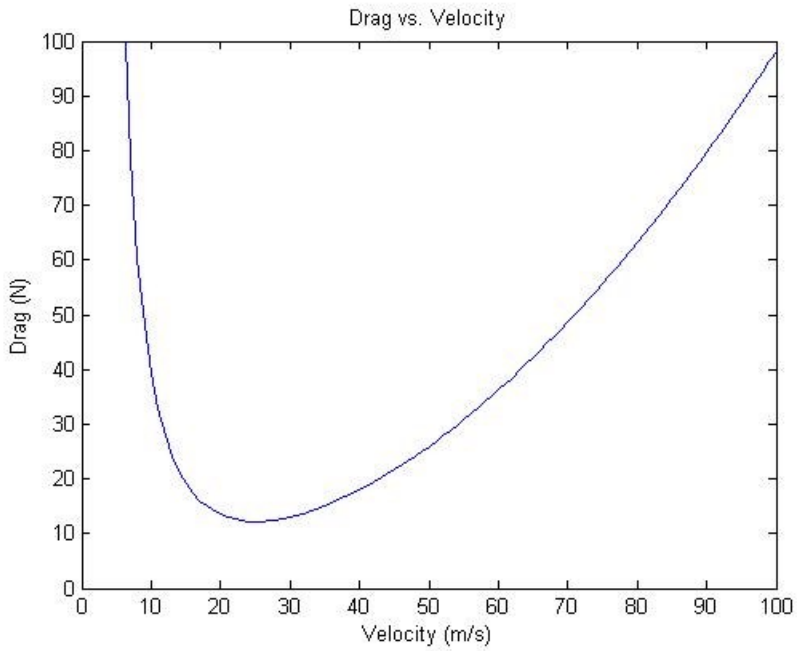

Figure 8: Drag vs. Velocity

The drag force vs. aircraft velocity is the typical shape that is expected and verifies the program is operating as intended and agrees with hand calculations. This plot also shows that the velocity for minimum drag is approximately 23 m/s. Dividing the drag force by the lift, gives the Lift/Drag ratio as a function of velocity. Figure 9 shows this function:

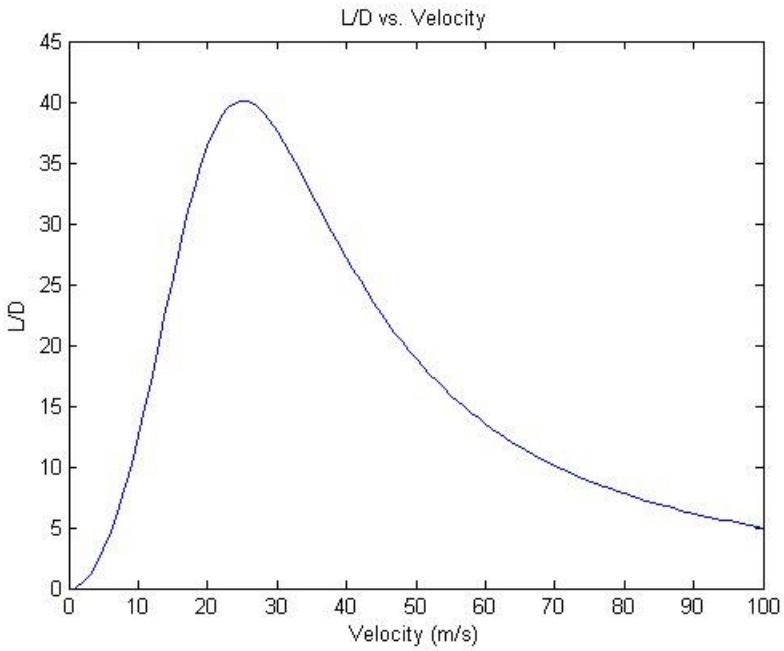

Figure 9: Lift/Drag vs. Velocity

From the graph the maximum L/D can be approximated about 40, which seems slightly high but these calculations neglect the tail section of the aircraft as well as many of the small inconsistencies in the aircraft which often can contribute a substantial amount to the total drag and therefore it is reasonable to expect that this number would be lower in reality.

2.3 Power Required for Flight

Since the airplane assumed to be in straight and level flight, the drag force of the airplane will be equal to the thrust provided by the power plant. Since the lab already had a motor pod designed and manufactured for a Cheetah A5530-9 brushless motor, a check of its suitability for use in the JetStreamer will be performed. The maximum power (P) rating

for the Cheetah motor is 2.2kW with a maximum motor efficiency of 88% but, since the motor will be operating over a wide variety of speeds, an average motor efficiency (η_{motor}) of 80% will be assumed. Additionally a propeller efficiency (η_{prop}) of 65% will be used from average Motocalc values for the proposed drive system. Therefore the actual power available (PA) to the airplane is:

$$PA = P * \eta_{motor} * \eta_{prop} = 2200 * 0.8 * .065 \approx 1140\ W \quad (6)$$

where P is power supplied to the motor. Since the thrust required is known for any velocity of the airplane, the power required (PR) for any velocity can be calculated by multiplying the thrust required at that velocity by the velocity. Figure 10 shows the power required vs. aircraft velocity along with a line showing the maximum power available from the Cheetah brushless motor.

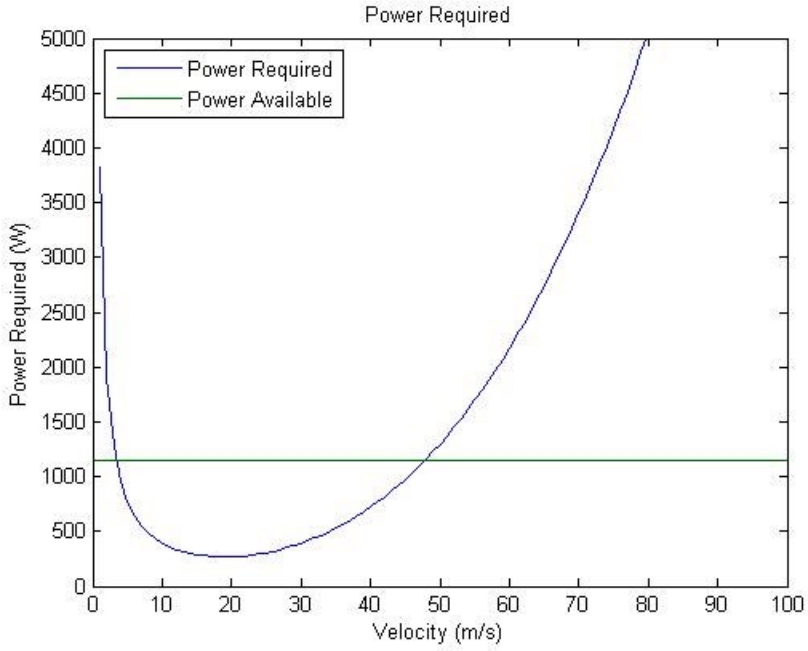

Figure 10: Power Required vs. Velocity

The intersection of the power required line and the line of power available gives the maximum straight and level velocity for the aircraft, and in case for the JetStreamer, it would be about 47 m/s. For initial testing, the Cheetah motor should be sufficient since it offers a reasonable flight. Additionally, there will most likely be some issues that need to be addressed before moving to higher velocities and therefore limiting the velocity initially will be advantageous. The slower response time of the aircraft at the lower speeds may also make it easier for the pilot to make corrections before the plane departs controlled flight.

When the aircraft has been sufficiently tested at lower speeds and it is decided the airplane is ready for high speed flights, the lab has a JetCat P200-SX Turbine engine that will be attached to the JetStreamer. The turbine can provide up to 230 N of thrust, which looking back to the Drag vs. Velocity graph (figure 8), the turbine should be able to provide ample thrust to achieve the desired speeds when the airplane is ready for the higher speeds and altitudes.

2.4 Climb Rate

The power available and power required are now known at all velocities, and from there the power available for climbing can be determined by subtracting the power required from the power available. Setting the power available for climbing equal to the weight of the aircraft multiplied by the vertical climb rate, the maximum climb rate at any velocity can be determined:

$$P_{climb} = PA - PR \Rightarrow V_{vert_{max}} = \frac{(PA - PR)}{m\ g} \quad (7)$$

Figure 11 shows the maximum climb rate vs. velocity.

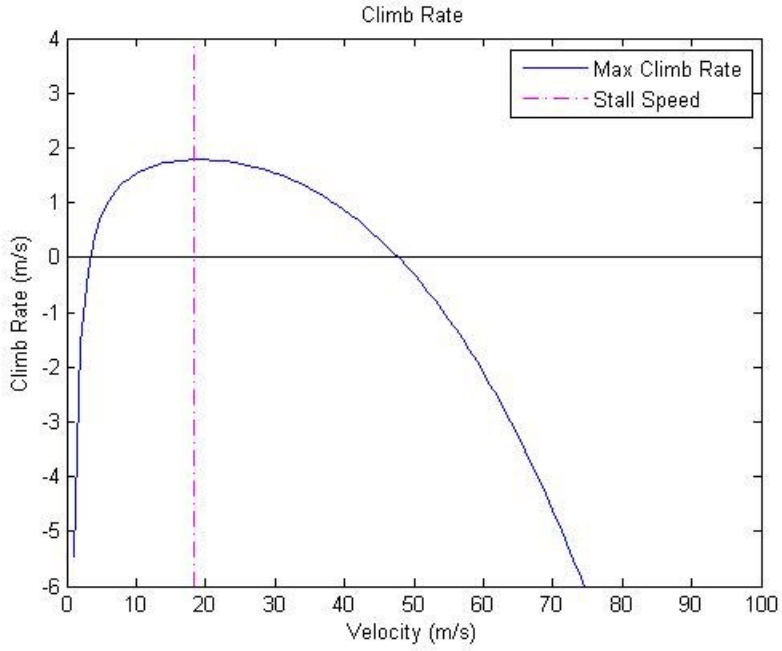

Figure 11: Climb Rate vs. Velocity for the Cheetah A5530-9 Electric Motor Driving a 20x13 Propeller

Figure 11 shows a maximum climb rate of about 1.8 m/s second. While this value is not incredibly high, it should be sufficient for preliminary testing of the aircraft.

2.5 JetStreamer Performance Summary

This basic analysis has shown that the aircraft's current configuration should allow for initial flight testing of the aircraft. The estimated parameters of the aircrafts performance with the Cheetah electric motor are as follows:

- Maximum lift to drag ratio of 40

- Stall velocity of 19m/s
- Maximum straight and level flight velocity of 47 m/s
- Maximum climb rate of 1.8 m/s

Once the basic test flights have been completed and the JetStreamer has proven to be airworthy, the electric motor can be replaced with the JetCat turbine engine for much higher performance and a wider operating envelope. Now that the basic aircraft design has been verified, work can begin on the details of the plane such as wing construction, control surfaces, etc.

3 Wing Design and Initial Testing

Since the wing is the most important part of an aircraft it was the first part the Lab chose to build. In order to achieve the desired aircraft weight with a wing aspect ratio of about 20, an entirely composite wing is essentially a must. In order to begin evaluating the construction techniques used to build a full size wing, some basic wing cross-section molds were constructed.

3.1 Preliminary Testing

To achieve the high strength to weight requirements of the aircraft, unidirectional carbon fiber prepreg will be used since it is the most effective solution due to its high stiffness, high fiber content, consistent mechanical properties, and it is much easier to build parts with on a larger scale than with vacuum infusion techniques. In order to build the JetStreamer out of carbon fiber prepreg, molds must be made for every part. To avoid any large, costly mistakes, test sections will be made first to ensure the process can produce the desired part quality. To begin, a set of test molds were made with just the airfoil shape in order to verify scale and basic processing techniques. The parting line for the molds was placed in line with the airfoil's chord. Therefore, one mold was the top skin profile and the other mold was that of the bottom skin profile. The first set of molds were made with an epoxy tooling board machined on Lehigh's 5-axis router. Figure 12 shows the first set of machined molds.

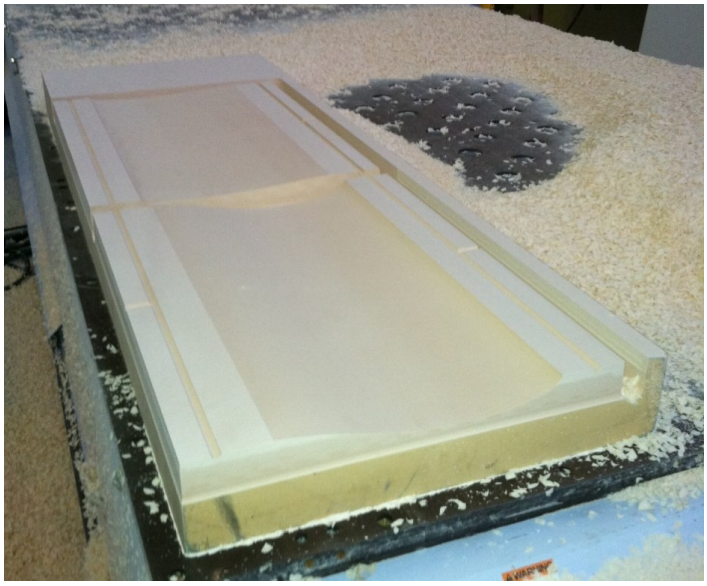

Figure 12: Machined Test Molds

The molds sealed with a thin layer of epoxy, and polished after the machining was complete. The molds were then mold released and ready for initial testing. For the first layup, two layers of a twill weave prepreg were used. Figure 13 shows the result of the first layup.

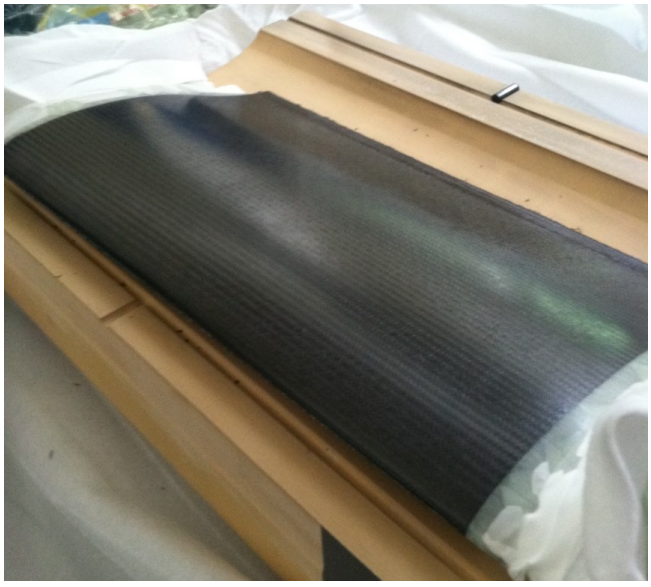

Figure 13: First Wing Section

The first test proved quality wing molds with a smooth finish could be produced and that high quality parts could be made from the molds. Since the first set of molds were made from an epoxy tooling board, the Glass Transition Temperature (Tg) of the tooling board was close to the curing temperature of the prepreg and as a result some minor deformations of the mold along the trailing edge. These mold deformations were caused by the plies being pinched between the mold halves while being subjected to high compressive forces while under vacuum. This showed future molds would need a tooling board with a Tg reasonably higher than the prepreg curing temperature in order to avoid any mold deformations.

3.2 Control Surface Considerations

The Lab strives to produce parts using one-shot manufacturing techniques and the JetStreamer wing is no exception. To achieve this, a couple of things needed to be incorporated into the final wing, a full wing spar, shear webs, and control surface recesses. The first challenge that was addressed was the control surface recesses since they would require inserts in the molds.

In general, parts should be built using the fewest molds and operations as possible. Each different component requires molds, trim fixtures, bonding jigs, etc. If creating an assembly from many components, then the required amount of tooling can become quite costly. With this consideration, the JetStreamer wing will be made in one shot, complete with upper and lower wing skins, upper and lower spar flanges, six internal shear webs,

and a trailing edge ready to accept ailerons and flaps. Figure 14 shows the basic layout of the main wing and the control surface profile.

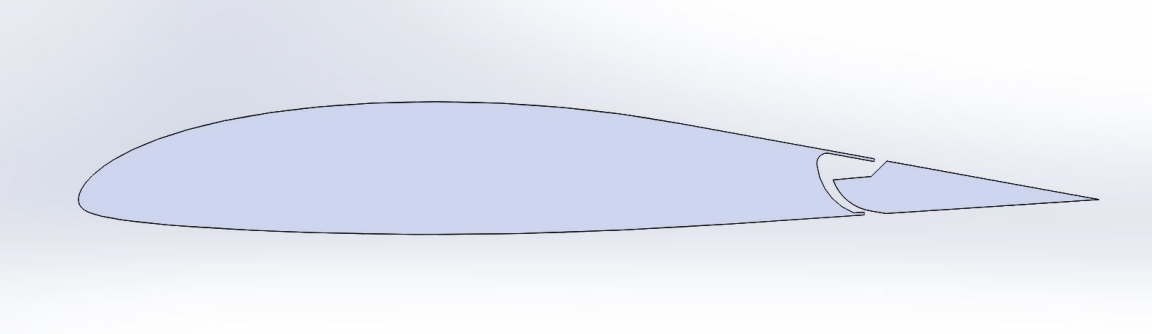

Figure 14: Wing and Control Surface Layout

This design allows for smooth airflow at all control surface deflection angles as well as placing the leading edge of the control surface ahead of the hinge line, which allows for mass balancing about the hinge.

From the desired wing and control surface profiles, a mold was designed. Figure 15 shows the mold design for the main wing with insert needed to create the trailing edge recess.

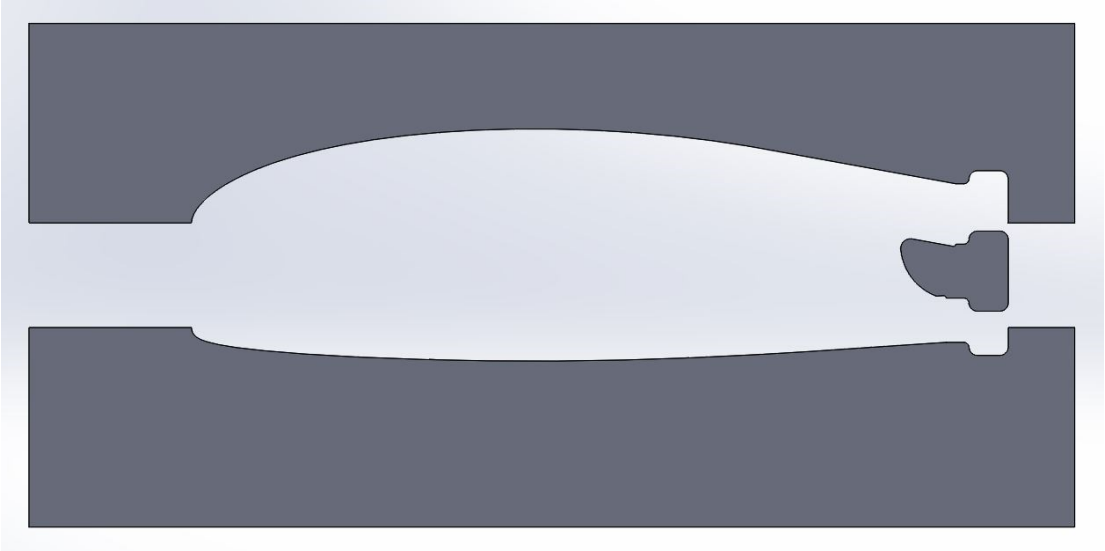

Figure 15: Wing Mold with Trailing Edge Insert

While the upper and lower mold halves could easily be machined all at once, the inserts required a slight bit more work and must be machined on all six sides. Because of their added complexity the inserts were machined out of aluminum on a HAAS VF-2 CNC mill with a jig which allowed them to be flipped over and located for additional machining.

3.3 Additional Testing

Once a new set of molds and the trailing edge inserts were machined, another test section could be created. The layup for this next test was done using only a unidirectional reinforcement. Since the wing skin will be responsible for taking a majority of the torsional load on the wing, a layup of [+45/-45/-45/+45] was chosen, which is torsionally very stiff. Figure 16 shows this layup in progress.

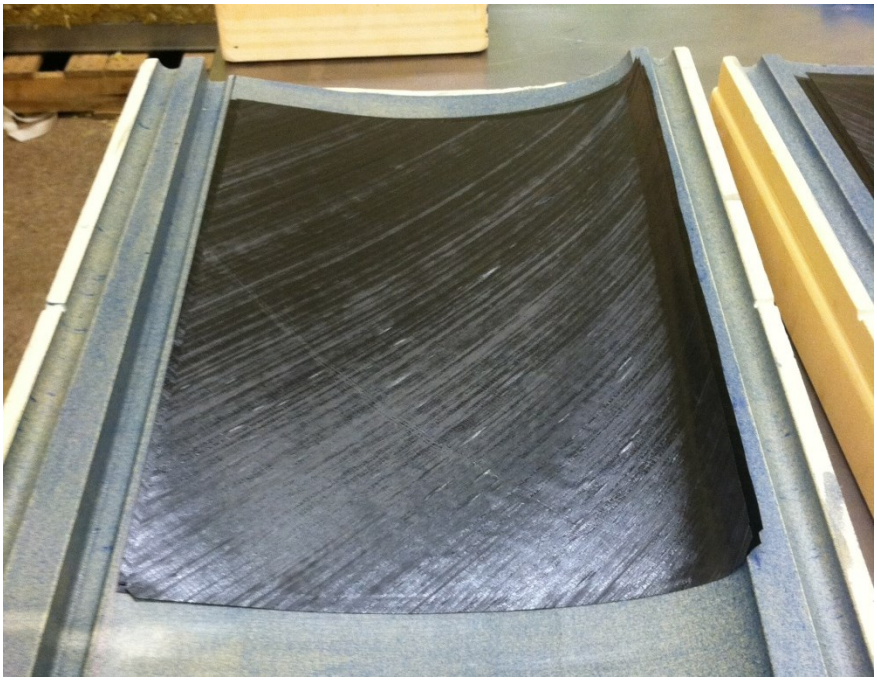

Figure 16: Wing Skin Layup

To create the trailing edge recess, the same ply schedule is laid on the aluminum inserts as well, which is shown in Figure 17.

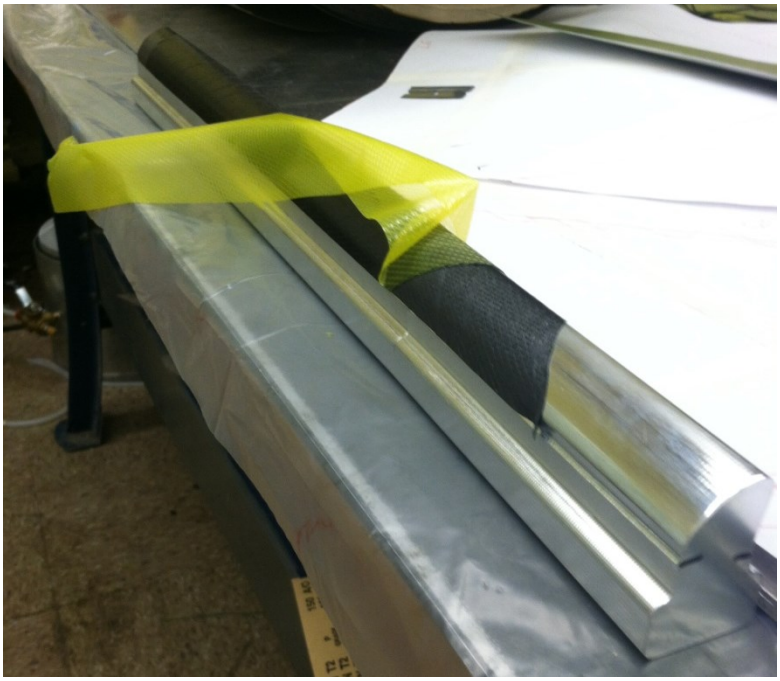

Figure 17: Trailing Edge Layup

Once all of the plies have been laid, the inserts are laid into the mold and then the other mold is placed on top to close the mold. After the part has been cured the two skin molds are separated, but the wing section and trailing edge inserts are stuck together. With the design of the inserts and some compliance in the carbon fiber, the inserts are freed by rotating them out of the trailing edge. Once the inserts have been removed, the finished part is all that remains; figure 18 shows the end wing for the test.

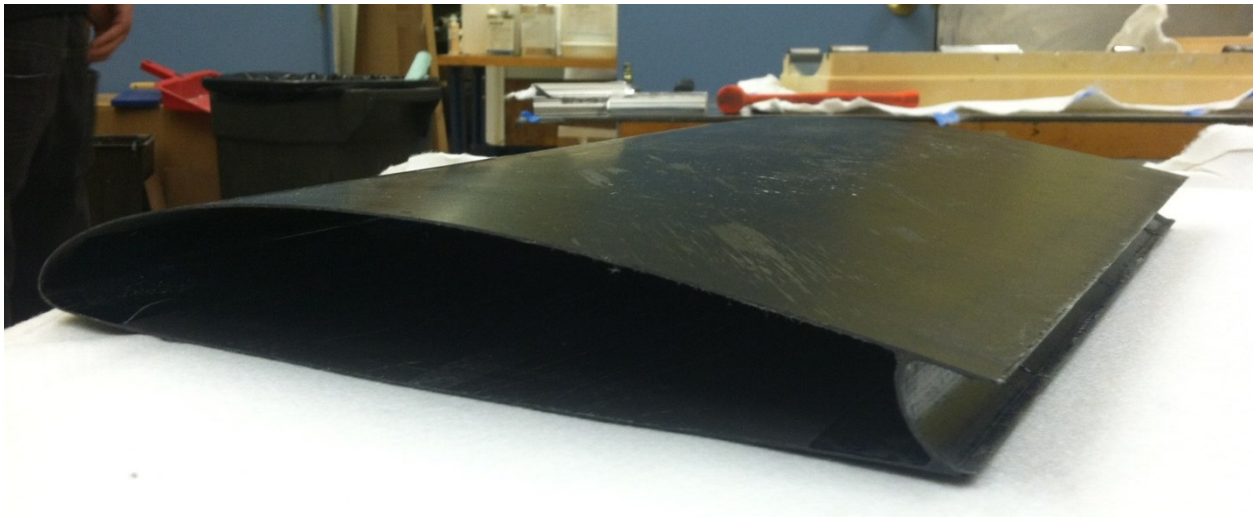

Figure 18: Finished Wing Section

In the figure above, it can be seen that the joints between the wing skins and the inserts came out very nicely and show no porosity or dry fibers. But one possible issue that will have to be considered in the future is the Coefficient of Thermal Expansion (CTE) differences between the molds and aluminum inserts. No adverse effects occurred at this scale of this test but they could be much more pronounced at a larger scale.

With these test it has been shown that a viable method for making control surface recesses as part of a one-shot process has been developed and should be easily scalable to the 6 meter wing as long as some precautions are taken with respect to CTE. With the control surface recesses completed, work can begin on developing the integrated wing spar.

3.4 Wing Spar Design

Using the basic design parameters of the aircraft, a wing spar can be designed using some rough approximations but should give reliable enough results for the purposes of this

aircraft. As a first order approximation, the lift profile will be considered to be a uniformly distributed load across the wing. This approximation is a conservative one since in reality the lift profile will be an elliptical distribution with zero lift at the wing tips, thus the calculations done with the uniform load will generate higher bending moments than reality. From the wing span including winglets (b), airplane mass (m) and load factor (n) a distributed load (q) can be calculated:

$$q = \frac{m\ g\ n}{b} = \frac{50 * 9.81 * 20}{6.5} \approx 1510\ N/m \tag{8}$$

With this information, a bending moment (M) can be determined at any point y on the wing, where y is measured from the wing centerline.

$$M = \frac{q}{2}\left(\frac{b}{2} - y\right)^2 = 755 * (3.25 - y)^2\ Nm \tag{9}$$

Plotting this function gives the following bending moment diagram in figure 19:

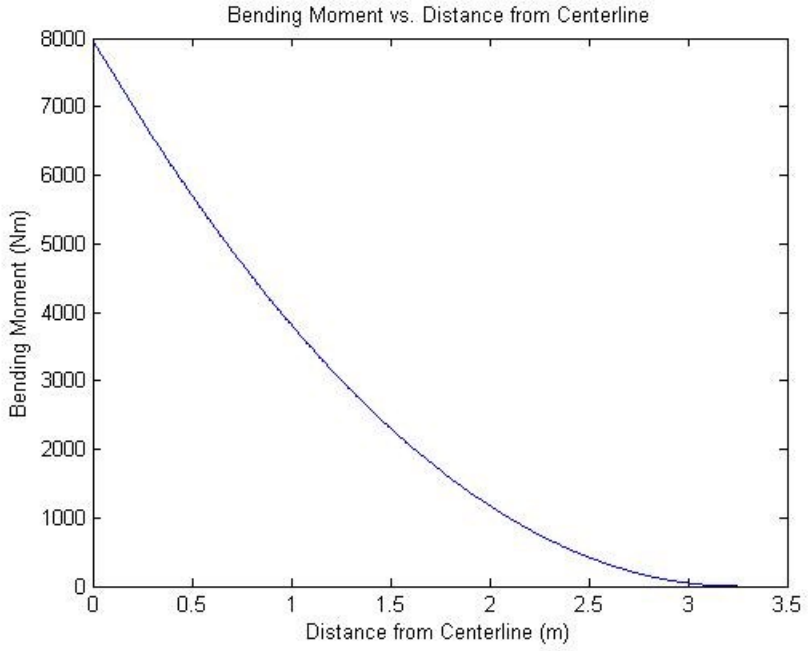

Figure 19: Bending Moment vs. Distance from Centerline

The spar will be constructed similarly to a box beam where the spar flanges will be made from unidirectional carbon fiber while the webs will be constructed with +/-45 degree fibers to take the shear loads. The flanges are integrated into the wing skins and therefore the beam height will be set equal to the airfoil thickness. Additionally since the web fibers are oriented in the +/-45 degrees directions, their strength contribution in the spanwise direction will be minimal and therefore neglected for the current spar calculations (but they must be sized appropriately to carry the shear forces in the beam). The wing spar can be approximated as a cantilevered beam for design purposes. It will also be assumed that the wing is similar to a beam that is linearly tapering in height equal to that of the wing. The remaining parameters needed now are that of the carbon fiber lamina. The carbon fiber prepreg system that will be used in the airplane's construction is Gurit's SE-84LV with T700 unidirectional fibers. This system gives the following properties:

- Fiber weight: ≈ 200 g/m²
- Tensile Strength ≈ 2840 MPa
- Tensile Modulus ≈ 129 GPa
- Compressive Strength ≈ 1187 MPa
- Ply Thickness ≈ 0.2mm

At this point, the forces, stress limits, and dimensions for the problem are set, now the required amount of carbon fiber in the flanges at any point in the wing can be directly calculated. With the current design information along with the lamina thickness a layup

schedule for the wing can be determined. For this design, beam deflection was disregarded and the wing spar was designed for strength.

Starting with the standard beam equation where d is the beam height and I is the area moment of inertia:

$$\sigma = \frac{Md}{2I} \tag{10}$$

Since the beam is linearly tapered, the value of d can be found at any point with the equation:

$$d = h_{root} - \left(\frac{h_{root} - h_{tip}}{\frac{L}{2}} \right) y \tag{11}$$

where h_{root} is the airfoil thickness at the root of the wing and h_{tip} is the wing thickness at the tip of the wing. If the flanges were rectangular with width (w) and thickness (t), the moment of inertia would be:

$$I_{spar} = 2 * \left(\frac{1}{12} w t^3 + A r^2 \right) \tag{12}$$

with r being the distance from the neutral axis to the flange's centroid. The flanges will be thin and therefore the first term can be neglected. Also assuming r ≈ d/2, the moment of inertia can be approximated as:

$$I_{spar} = \frac{A_{flange} d^2}{2} \tag{13}$$

Where A_{flange} is the cross-sectional area of one flange. Combining the equations and rearranging to solve for the required flange area as a function of wing location (y) yields:

$$A_{flange} = \frac{q\left(\frac{b}{2} - y\right)^2}{2\sigma\left(h_{root} - \left(\frac{h_{root} - h_{tip}}{\frac{L}{2}}\right) * y\right)} \tag{14}$$

The spar width was set to be 90mm wide and, from there the required ply thickness can be determined everywhere along the wing. A compressive strength of 700 MPa will be used for the unidirectional fibers, this strength is more likely to be achievable than the considerably higher value recorded in the datasheets.

The wing is designed for either a positive or negative 20 g load and therefore it is reasonable expect beam fail in compression in either flange and therefore the 700 MPa compressive strength will be used as the failure strength for the beam since it is the lower of the two failure strengths. A MATLAB script was created to use the previous equation to determine required ply thickness throughout the wing and generate the layup schedule for the spar. This script is given in Appendix C.

When determining required number of plies, the program decreases the flange ply width by 2mm for each successive ply added to the spar to help create a smooth transition to the spar from the wing skin. The program also always rounds up the number of required plies to the nearest integer, rather than tapering the ends of the plies. Finally the program plots the required number of plies versus location along the wing from the centerline. From the given design parameters, the following plot was generated:

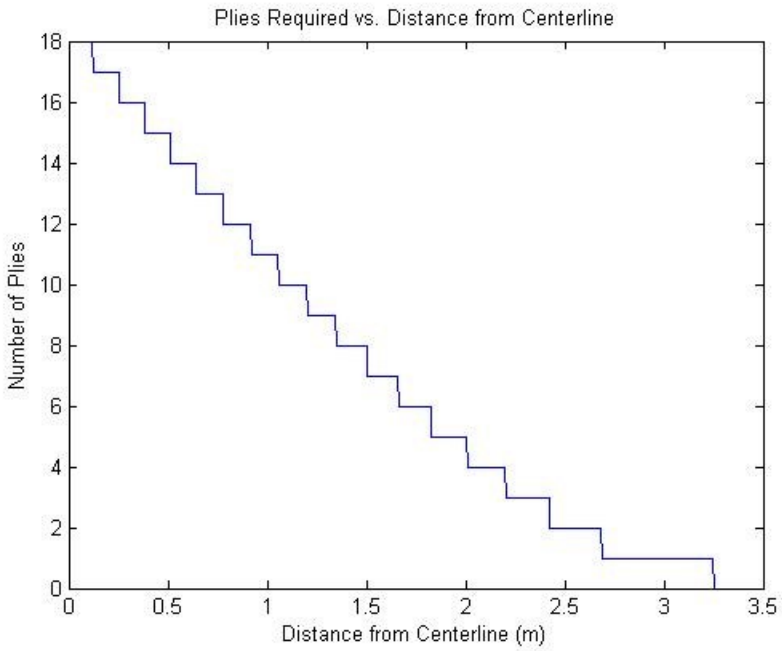

Figure 20: Plies Required vs. Distance from Centerline

The number of plies essentially follows the shape of the bending moment but deviates slightly due to the decreasing beam height farther away from the centerline as well as the decreasing ply width of each successive ply.

3.5 Wing Shear Webs

Now that the spar flanges have been designed, the webs of the spar must be designed in order to carry the shear load. To begin, the shear stress (τ) at any point along the beam can be calculated using the following equation:

$$\tau = \frac{V}{d\,t} \tag{15}$$

Where V is the shear force, d is the web height and t is the web thickness. Since the load on the wing is assumed to be evenly distributed, the shear force can be calculated using:

$$V = \frac{n\ m\ g}{2}\left(1 - \frac{2y}{b}\right) \tag{16}$$

To determine the maximum shear strength of the webs, a stress transformation must be done to put the stresses along the fiber directions. Since the webs must take the shear load and not the tensile load, the layup will be [+45/-45/-45/+45], with the 0° direction being the spanwise. This layup has high shear strength and stiffness, along with being balanced and symmetric. The latter tends to lead to less deformation after cure than non-symmetric layups.

From Mohr's circle a pure shear stress can be rotated to give tensile and compressive strength of equal magnitude along the principle axis. Thus, with the webs, a shear stress will cause a tensile stress along the +45° and a compressive stress along the -45°. This can be reversed depending on the shear force direction but the net effect is the same. Since a ply essentially only carries forces along its fiber direction, then the effective thickness is only half of the laminate thickness. Once again, using the 700 MPa compressive strength of the prepreg, taking into account the effective thickness, and using Mohr's circle, the shear stress limit becomes 350 MPa.

As before, d will be assumed to be linearly tapered from the wing centerline. Using the program for the spar design, V, b can easily be computed and using the shear strength, the required web thickness can be computed. Figure 21 shows the MATLAB program results for the required web thickness.

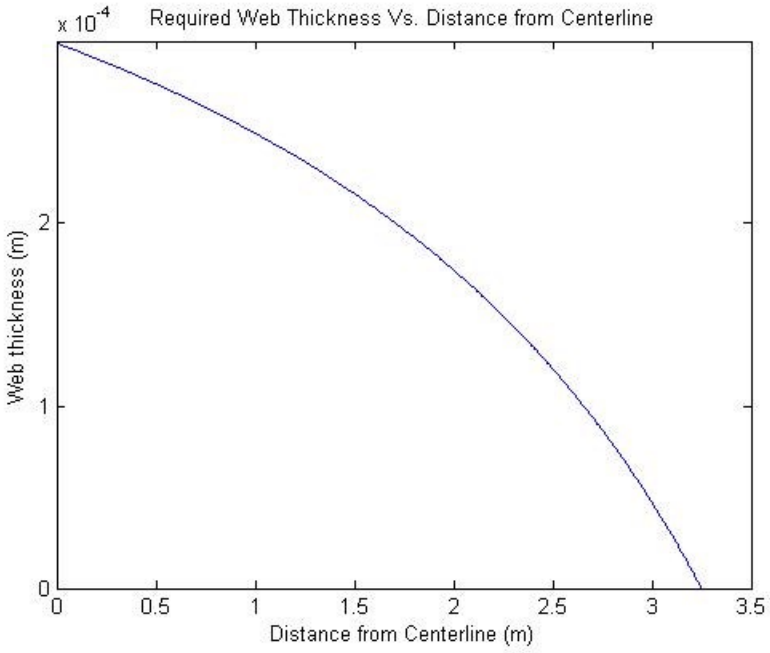

Figure 21: Required Web Thickness Vs. Distance from Centerline

From the figure, it can be seen that the wing only needs about 0.30 mm of web thickness to carry the shear load. Considering the minimum symmetric and balanced layup for a wing skin that has a thickness of 0.8 mm and thus a total centerline thickness of 1.6 mm, the wing should be nowhere near shear failure in the webs. However, this analysis does neglect shear buckling effects and is beyond the scope of this analysis.

While just the thickness of the skins provides sufficient strength to handle the shear load of the wing, the skin is still very flimsy. With the earlier test specimens, the profile can easily be deformed by hand, and needs to be stiffened to retain its proper aerodynamic shape. A structural core could be used in the wing but this can be quite heavy and also difficult to manufacture. The mass of the foam core can be estimated as follows. The skin can be assumed be twice the planform area (S). Diab HT61 foam is suitable since it is the lightest available high temperature structural foam from Divinycell. It has a density (ρ) of

65 kg/m³. As a reference, a 3mm core thickness (t) will be used as a first approximation. Thus an approximation of the core weight would be:

$$m_{foam} = V_{foam} * \rho_{foam} = 2\,S * t * \rho_{foam} = 2 * 1.8 * .003 * 65 \approx 0.70\,kg \quad (17)$$

Though when using a foam core, a glue film must be applied on both sides of the core in order to have sufficient bond strength between the skin and core. The glue film area can then be assumed to be four times the planform area. Using a 100 g/m² areal weight glue film, the weight can be estimated by:

$$m_{film} = A_{film} * \left(\frac{\rho}{t}\right)_{film} = 4\,S * \rho_{foam} = 4 * 1.8 * .100 \approx 0.72\,kg \quad (18)$$

Thus a total weight of 1.42 kgs is needed to stiffen the skin using a foam core. A different way to support the skins is with a number of internal webs, which would greatly reduce the unsupported length of the wing skins. Figure 22 shows a sketch of the internal structure with the numbers being used to identify the different sections of the internal structure.

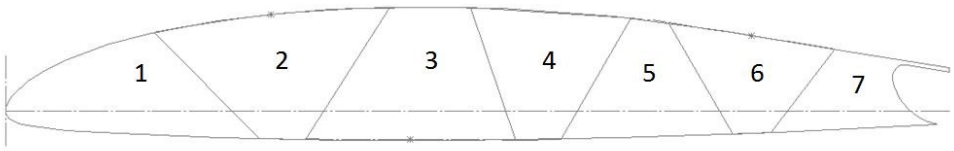

Figure 22: Wing Internal Structure

The total web lengths in figure 22 are about 0.43 times the length of the perimeter of the section. Assuming this shape is kept throughout the length of the wing and the same

layup is used in the webs as the skin, a weight estimate for the web weights can be calculated as follows:

$$m_{webs} = 2\,S * \ .43 * t_{skin} * \rho_{skin} = 2 * 1.83 * 0.43 * .0008 * 1000 \ \approx 1.25\ kg \quad (19)$$

The web mass estimatiion is slightly low since it does not account for overlap of the fibers onto the wing skin. In the end, both designs will most likely be similar in mass.. One major advantage of the web structure over the foam core is that the webs can be integrated into the wing layup with very little extra work whereas the foam core would require extra steps for curing the outer skin, forming and installing the foam core, continuing the layup, etc. Thus the web structure adds to ease of a one-shot manufacturing process for the wing.

The Lab decided that if a viable process could be created for the wing with the internal web structure that it would be quite advantageous to pursue the opportunity. Using the test mold already created from earlier, the evaluation of the manufacturing methods for the web structure could begin.

3.6 Web Manufacturing Testing

To create the webs and have them placed in the correct location, some form of a mold or place holder must be used. The web molds must be removable because they would otherwise add pointless weight in the wing. Removing the molds becomes particularly challenging when the wing is quite long while the openings at the wing tips are quite small. Essentially the internal molds must be disposable and dissolved or in some other way removed through a small opening. Polystyrene foam seemed to be reasonably well

suited for the role. If the wing is cured at temperatures above 100 °C the polystyrene will begin to shrink, particularly under vacuum. If the wing is cured at lower temperatures, the polystyrene would keep its shape after curing. The foam would then have to be, for example, be chemically dissolved using some form of solvent. Though when using the solvent, extra steps would have to be taken to safely dispose of the byproducts afterwards.

To begin testing, a set of polystyrene molds were cut with the shapes of sections 2, 4, and 6 as shown in figure 22. The foam molds are then placed inside lay-flat vacuum bags and evacuated in order to make the bag the same shape as the mold. Once these were prepared a test layup could begin.

This test starts similarly to the previous test, in that the first two skin plies are laid and debulked onto the mold surface. But this test has the addition of integrated spar caps, which are built into the wing skins. After the first two layers are in place, the wing spar is laid on the skin plies. Figure 23 shows the layup after the spar plies have been laid in.

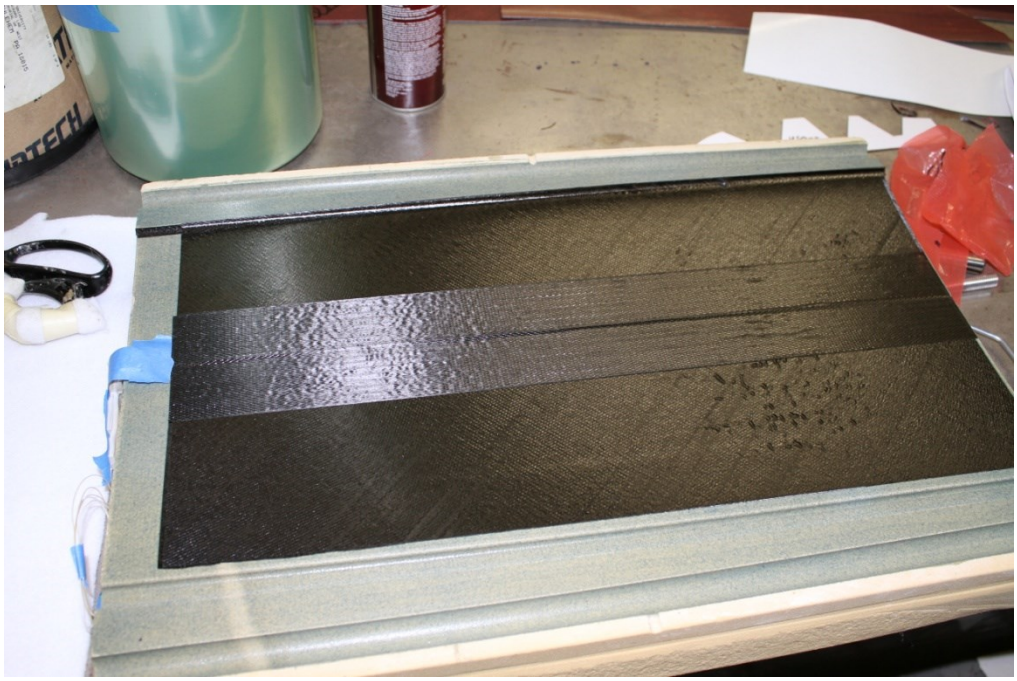

Figure 23: Spar Layup

Then the other two skin plies are laid on top of the wing spar and previous skin plies. This layup maintains symmetry and balance in the wing skin, which will help avoid any twisting or other odd deformations during the cure, as well as helps avoid odd deformation modes of the wing under load. After this point the foam molds are laid into the top mold and stuck down to the plies currently on the mold. Additionally, peel ply strips are placed on the top and bottom of the foam molds to help with air evacuation once under vacuum. Figure 24 shows the foam pieces in place and ready to begin layup of the webs.

Figure 24: Placement of Foam Molds

The layup of the webs can now begin. The webs have the same layup, [+45,-45,-45,+45], as the wing skin. The layup is done with separate plies for each of the three foam molds and when the plies are placed on top of the wing skin, symmetry and balance of the laminate is still maintained even in the joints. Figure 25 shows the web plies after being laid, debulked, and ready to continue with creating the control surface recesses.

Figure 25: Finished Web Plies

The foam molds are also made slightly oversized so that when the molds are closed, contact is guaranteed between the web plies and the bottom skin plies on the other mold. The trailing edge inserts and their associated plies are now placed into the mold and more lay-flat vacuum bags are placed in the four remaining sections of the mold and, by doing so, pressure can be applied to both sides of the webs while under vacuum and compact the plies. The mold is then closed, wrapped in breather and a vacuum bag is placed around the entire mold and sealed to the outside of the seven internal vacuum bags. The inside of the inner bags is allowed to be at atmospheric pressure and essentially inflate inside of the mold cavity due to vacuum being applied to the mold. Figure 26 shows the mold sealed up, under vacuum, and ready to be placed in the oven.

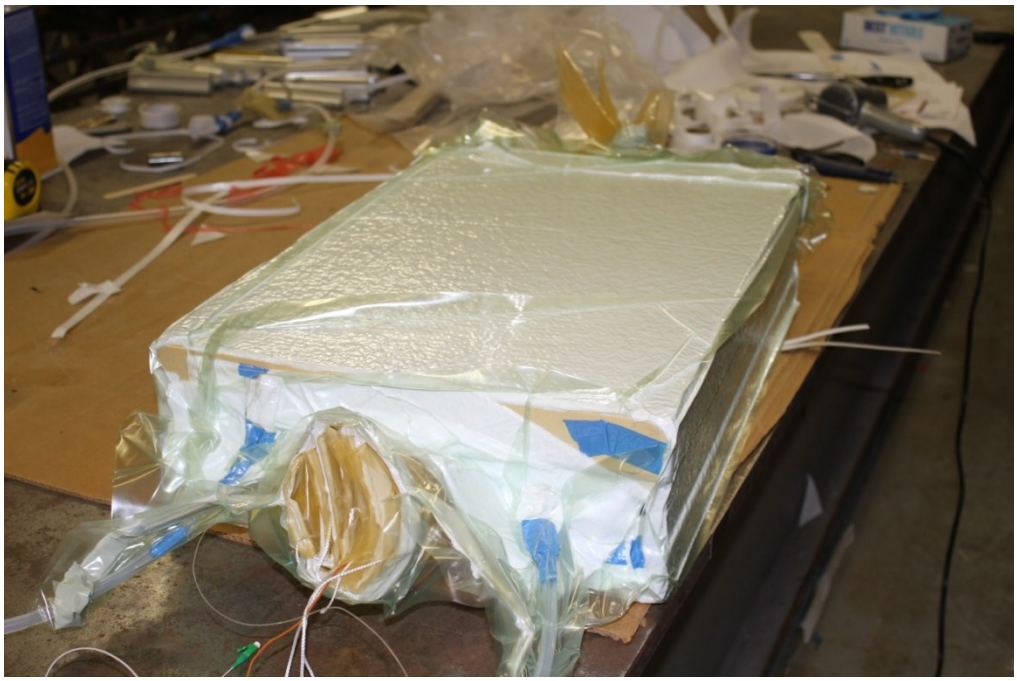

Figure 26: Test Mold Under Vacuum

The mold is then placed in an oven and cured at 85°C for 24 hours. After curing, the molds are removed from the oven, separated and the finished part is released from the molds. Since the cure was below 100°C, the foam molds showed very little distortion and were able to be slid out of the side of the test section, but this is only possible since the section is tapered in only one direction. The foam molds were in surprisingly good condition and could be used for future. Figure 27 shows the finished part once all of the bagging materials were removed.

Figure 27: Finished Wing with Internal Structure

The webs ended up surprisingly straight even though during the layup the plies would end up with some curvature. The part also shows good bonding of the webs to both the top and bottom skins with no major defects in the joints but some minor surface defects can be seen on the skins where the webs meet the outer skin. Figure 28 shows some of the surface defects that were typically seen with the addition of the webs.

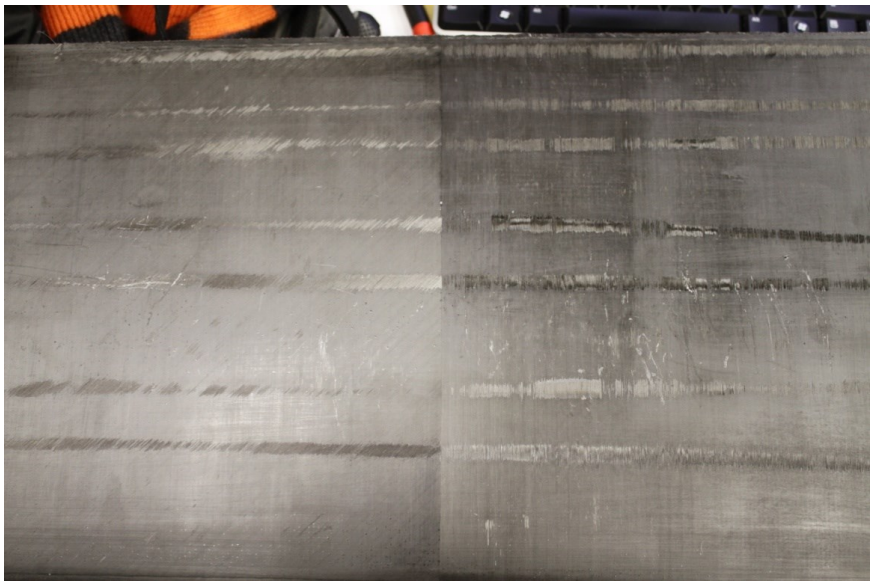

Figure 28: Typical Skin Defects

These defects line up with the joints between the skin and the webs and are somewhat expected since vacuum bags have difficulties working themselves into the tight corners and very little force can be applied in them since the area is quite small. The use of an autoclave could reduce this. Figure 28 was from a test to determine if the addition of fiber layers in the chord direction could reduce or eliminate these defects, but it was determined to have a small impact on part quality and added undesirable weight.

In the end, the webs substantially increased the stiffness of the wing skins and the end product was deemed sufficient for the purposes of this.

3.7 Wing Torsional Stiffness

The next step along the process is determining if the wing will have adequate torsional stiffness to negate aeroelastic effects such as divergence, flutter, and control reversal. For the purpose of this paper only control reversal will be addressed.

Since the wing is constructed out of unidirectional carbon fiber, the analysis will start with the minimum symmetric and balanced layup for high torsional stiffness [+45,-45,-45,+45]. To determine the torsional stiffness, the shear modulus of the skin must be known. The datasheet only provides the uniaxial tensile modulus (E_1) in the fiber direction. Through the use of tensor transformations, the shear modulus (G_{12}) can be determined for the skin assuming a rotated ply. Since stiffness (Q_{ijkl}) is a fourth order tensor, its components in a rotated system are:

$$Q'_{ijkl} = (\boldsymbol{e}'_i \cdot \boldsymbol{e}_p)(\boldsymbol{e}'_j \cdot \boldsymbol{e}_q)(\boldsymbol{e}'_k \cdot \boldsymbol{e}_r)(\boldsymbol{e}'_l \cdot \boldsymbol{e}_t)Q_{pqrt} \tag{20}$$

where $\boldsymbol{e}_p$, $\boldsymbol{e}_q$, $\boldsymbol{e}_r$. $\boldsymbol{e}_t$ are the unit vectors along the original $\boldsymbol{x}_1$, $\boldsymbol{x}_2$, $\boldsymbol{x}_2$ and the $\boldsymbol{e}'_i$, $\boldsymbol{e}'_j$, $\boldsymbol{e}'_k$, $\boldsymbol{e}'_l$ are the unit vectors in the rotated coordinate system axes $\overline{\boldsymbol{x}_1}$, $\overline{\boldsymbol{x}_2}$, $\overline{\boldsymbol{x}_2}$. As a first approximation, it may be assumed that all stiffness components except Q_{1111} are equal to zero and that

$$Q_{1111} = E_1 \tag{21}$$

if Poisson effects are neglected. Then using equations 20 and 21 gives the shear modulus of the rotated system:

$$Q'_{1212} = G_{12} = E_1 \sin^2\theta \cos^2\theta \tag{22}$$

where θ is the angle of rotation. Thus if a ply is rotated 45°, the shear modulus is:

$$G_{12} = 129 * \sin^2(45)\cos^2(45) \approx 32\ GPa \tag{23}$$

This shear modulus if for a single ply rotated 45°, but since the transformation is an even function and the laminate is a balanced layup of only +45 and -45 plies, the skin shear modulus is the same as the individual ply shear modulus of 32 GPa. Now that the shear modulus is known for the skin, the torsional stiffness calculation can continue. The wing

will be modeled as a thin-walled linear tapered noncircular tube in torsion. Beginning with equation for angular deflection (θ) of a noncircular tube with an applied torque (T) at the end of the tube:

$$\theta = \frac{T\ L\ U}{4\ GA^2\ t} \tag{24}$$

Where L is length of the tube, U is the length of the median boundary, A is the cross-sectional area, and t is the wall thickness. In this case, U and A will be a function of y along the wingspan, and while in reality T would be a function of y, as a simplification, T will be a moment that is only applied at the end of the wing. One advantage of only applying the moment only at the end of the wing is that load can be replicated in real tests, whereas a distributed moment would be more difficult. Assuming a small length dy will give a small deflection dθ. Thus:

$$d\theta = \frac{T\ U(y)}{4\ GA(y)^2\ t}\ dy \tag{25}$$

To continue, the functions of U(x) and A(x) must be determined. These values can be approximated from the CAD model of the wing. At the root of the wing, the cross-section area is .0109 m² and has a perimeter of .650 m. At the tip, the cross-sectional area is .0027 m² with a perimeter of .345 m. Assuming that the perimeter scales linearly with distance from the center of the wing, while the area will scale with the second power. Thus some close approximations to the perimeter and area are the following:

$$A(x) = 0.0109 * \left(1 - 0.5\frac{y}{L}\right)^2 \quad U(x) = .65 * (1 - 0.47\frac{y}{L}) \tag{26}$$

Checking the endpoints of each of the approximations agrees with the CAD model. Integrating both sides of equation 25 gives the following

$$\int d\theta = \int \frac{T\,U(y)}{4\,G\,A(y)^2\,t}\,dy \;\Rightarrow\; \theta = \frac{T}{4\,G\,t}\int_0^a \frac{U(y)}{A(y)^2}\,dy \tag{27}$$

Where a is any point along the wing measured from the centerline. Using WolframAlpha to compute this integral gives:

$$\theta = \frac{T}{4\,G\,t}\left[\left(\frac{L^3(5361.5\,L - 2571.33\,a)}{(L-0.5a)^3}\right) - \left(\frac{5361.5\,L^4}{L^3}\right)\right] \tag{28}$$

Rearraging for torsional stiffness at the wing tip (a = 3m) and using G = 32 GPa, L = b/2 = 3m, t = .0008m gives:

$$\left(\frac{T}{\theta}\right)_{wing} \approx 2012\,\frac{Nm}{deg} \approx 115280\,\frac{Nm}{rad} \tag{29}$$

This calculation represents a worse case loading of the wing since there will be a distributed moment along the wing and therefore would result in smaller deflections. As a reality check for this answer, the torsional stiffness calculations were done for a constant cross-section thin-walled tube with the cross-section of the root and another with the cross-section of the tip both of equal length to the wing (3m). The following results were obtained:

$$\left(\frac{T}{\theta}\right)_{Root} \approx 6196\,\frac{Nm}{deg} \quad and \quad \left(\frac{T}{\theta}\right)_{Tip} \approx 715\,\frac{Nm}{deg} \tag{30}$$

Now using this information and a moment generated by the wing with full control surface deflection, calculations should give a rough idea if control reversal could be an issue. Starting with the definition of the moment coefficient:

$$C_m = \frac{M}{\frac{1}{2}\rho\,v^2\,S\,c} \tag{31}$$

From the Theory of Wing Sections [4], the moment coefficient can be approximated as:

$$C_m = \delta\left(\frac{\partial C_m}{\partial \delta}\right) \tag{32}$$

With a control surface chord percentage of 22%, $\frac{\partial C_m}{\partial \delta}$ is approximately 0.65. Assuming a small control surface deflection (Δδ), the moment coefficient is:

$$C_m = \delta(0.65) \tag{33}$$

Continuing and using the aircraft parameters, the moment generated per deflection can be calculated as:

$$\frac{M}{\Delta\delta} = \frac{\partial C_m}{\partial \delta}\left(\frac{1}{2}\rho\, v_{max}^2\, S\, c\right) = 0.65 * \frac{1.23}{2} * 135^2 * 1.8 * 0.292 \approx 3829\frac{Nm}{rad} \tag{34}$$

This value is for the entire wing, therefore since it is symmetric about the centerline there will be a moment of about 1914 Nm/rad per side. This is also a distributed moment along the entire wing and would result in smaller deflections than if applied only at the tip.

For a 22% control surface chord percentage, the control surface effectiveness ($\frac{\Delta a_0}{\Delta \delta}$) is approximate 0.45.The effective change in angle of attack per control surface deflection ($\frac{\Delta a}{\Delta \delta}$) can be computed by:

$$\frac{\Delta a}{\Delta \delta} = \frac{\Delta a_0}{\Delta \delta} - \frac{M}{2\,\Delta\delta}\left(\frac{\theta}{T}\right)_{wing} = 0.65 - \frac{3829}{2} * \frac{1}{115280} \approx 0.63 \tag{35}$$

Therefore the wing should provide adequate torsional stiffness to avoid control reversal since the effective change in angle of attack is positive and indicates C_l will increase with control deflection as expected. Additionally, it is expected the wing will have an even higher torsional stiffness due to the addition of the webs which create multiple torsion

cells in the wing structure, but need not be considered since the wing has already shown adequate torsional stiffness without them.

4 Wing Mold Design and Construction

Now that preliminary design calculations have been completed along with the initial test specimens showing positive results, work can begin on constructing a full size wing for the JetStreamer in a one-shot process. The same techniques will be used for the full size wing as was used on the small scale tests.

4.1 Mold Design

To begin, a mold material must be chosen, and after the preliminary tests, it was apparent that most epoxy tooling boards do not have a high enough glass transition temperature for the current process. An alternative option is high temperature polyurethane tooling boards, which can have a much higher Tg. The weight of a 6+ meter mold can also become a problem, especially if it must be moved by hand. Another consideration is cost, which is typically proportional to density. So in order to minimize cost and allow for easy handling, a low density tooling board is desired. But as density decreases, so does strength and machined surface finish.

It was decided to use General Plastics FR4718 due to its high glass transition temperature of 220°C and its relatively low density of 288 kg/m³. One problem with the FR4718 is it does have a fairly high Coefficient of Thermal Expansion (CTE) of 48*10^-6 1/K which

is about twice that of aluminum and about four times that of mild steel. This will be a concern since currently the trailing edge inserts are aluminum and some methods of minimizing this impact will need to be used.

Also to create a mold over 6 meters in length purely out of tooling board would be quite costly and would have fairly little strength. For that reason, it was decided to create fairly thin molds out of the tooling board and support them with a steel structure that provides the strength and stiffness required for the long molds. To start with, a basic layout of the molds must be created. The molds must also account for the wing's 4 degree dihedral that begins 1.8m from the wing centerline. Figure 29 shows the layout of the molds and the wing pattern used to create the mold shapes. The profile used for the wing is essentially the same as in the previous tests. The aluminum trailing edge inserts will still be used as well but will have to be sized appropriately to deal with the high thermal expansion of the molds.

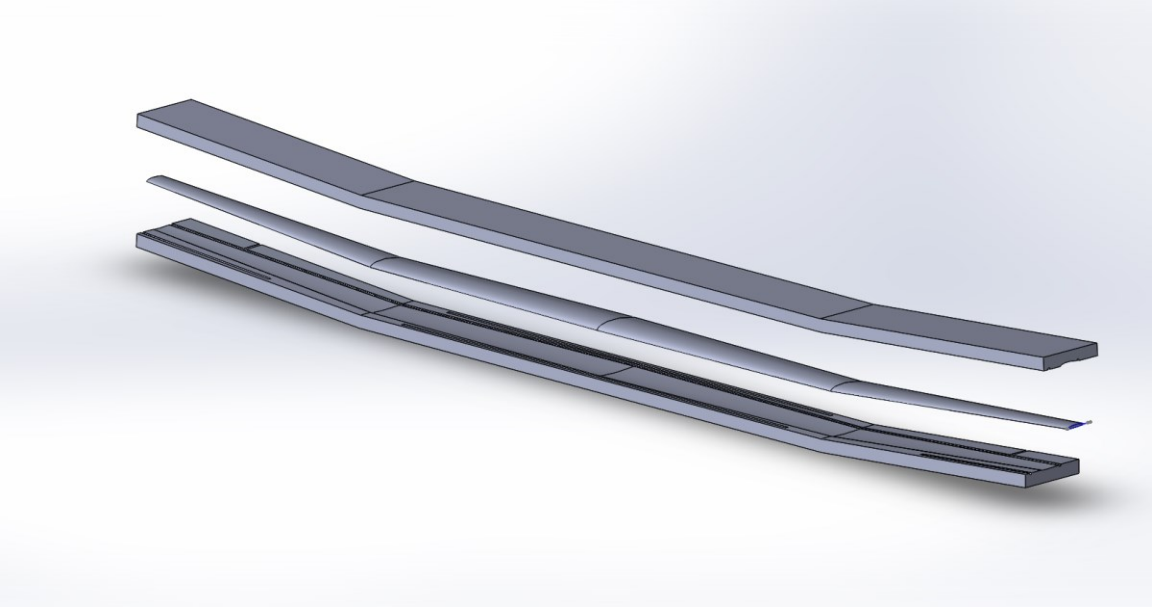

Figure 29: Wing Mold Layout including the Wing (in the center)

Using a maximum cure temperature of 120°C and assuming a room temperature of about 20°C, an estimate of the mold expansion can be made. It will be assumed the mold is pinned in the middle and therefore the free length will be 3.25 meters. Thus the mold expansion is:

$$\Delta L = L * \Delta T * CTE = 3.25 * (120 - 20) * 48 * 10^{-6} = 0.0156\, m \quad (36)$$

This shows that mold expansion is considerable of over the mold length. Performing this analysis for both aluminum and steel yields expansions of 0.0085m and 0.0040m respectively. The steel support structure must be allowed to move relative to the molds in order to avoid stressing the mold. Now the problem is that ample support of the molds is needed in order to maintain the shape but it must also be somewhat isolated from the steel structure due to the CTE mismatch.

4.2 Design of the Mold Support Structure

Since the molds will need a long, lightweight and stiff support structure, a truss frame will be designed to support the entire length of the wing molds. The truss will be manufactured using 25mm steel square tubing with 1.5mm walls. For ease of handling, the truss structure should not extend beyond the molds. With the wing molds being 450mm wide, a truss width of 375mm allows the molds to protrude past the sides of the truss on either side. For the ease of manufacturing the height of the truss will be 375 mm as well. The distance measurement between the tubes will be from center point to centerpoint. For the following stiffness calculations, the triangulation tubes in the middle will be neglected.

Considering only the top and bottom tubes, the moment of inertia can be calculated. The tubes will be located fairly far away from the neutral axis, and therefore only the contributions from the parallel axis theorem will be used. Thus the truss's moment of inertia can be approximated as the following:

$$I_{truss} = 4\,A\,r^2 = 4 * (4 * .025 * .0015) * \left(\frac{.375}{2}\right)^2 = 21.1 * 10^{-6}\ m^4 \qquad (37)$$

Where A is the material area of the tube and r is the distance from the tubes centroid to the neutral axis. Also, assuming a typical steel Young's modulus (E) of 200 GPa, a deflection can now be determined using the standard solution for a simply supported beam in bending.

As a worst case scenario, the mold structure will be assumed to be simply supported at either end; therefore a beam length (L) of 6 meters will be used. Finally, a distributed load (ω) can be calculated from the density and a mold width of 450mm and height of 75mm giving a distributed load of approximately 100 N/m. Therefore the standard solution for deflection of a beam with a distributed load is:

$$\delta_{max} = \frac{5\,\omega\,L^4}{384\,E\,I} = \frac{5 * 100 * 6^4}{384 * 200 * 10^9 * 21.1 * 10^{-6}} = 0.0004\,m \qquad (38)$$

While this deflection is quite low, the distributed load could be increased by a factor of 5 when the other mold structure is placed on top of it to close the mold. But even in this case, deflection would only be about 2mm which is more than acceptable for scale of the molds. Also, in reality, the supports will be located farther in on the mold support structure and would result in smaller deflections. Now that the dimensions for the truss

structure have been set, a solid model can be created and from there a cut list can be made for the structure. Figure 30 shows the final truss design.

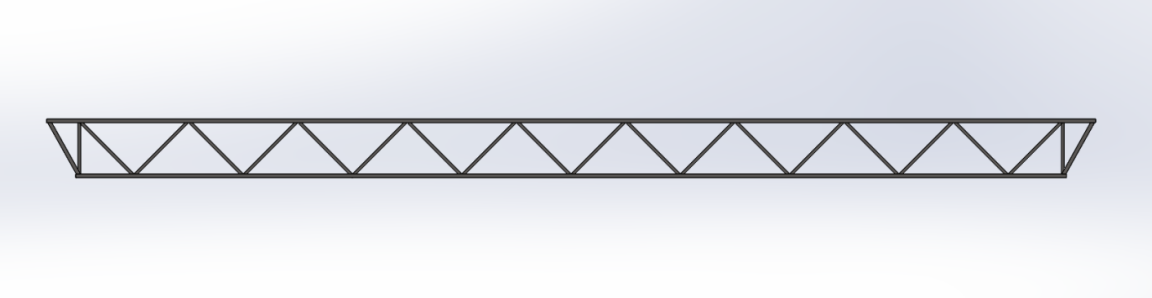

Figure 30: Mold Support Truss

The support structure has now been designed, but a method for allowing movement between the mold and the frame while still giving the mold ample support needs to be created. To accomplish this, a flexure will be designed that goes from the support truss to the mold. This flexure will allow movement along the length of the truss but will still provide high stiffness in the transverse and vertical directions. Since the mold will have a pin support at the center of the molds, the structure is essentially statically determinate, if the force from the flexures is considered negligible.

4.3 Mold Support Flexure Design

For the design of the flexure it will be assumed that the load case is two fixed walls that have the supports offset. Figure 31 shows the type of deflection that is expected.

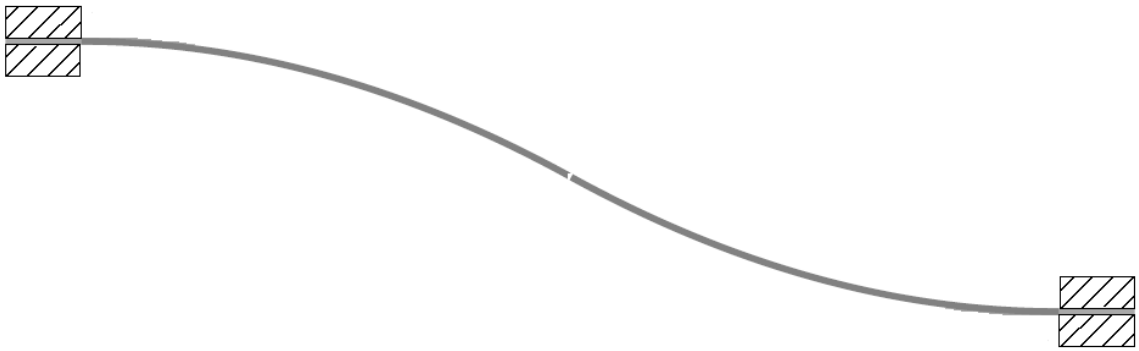

Figure 31: Flexure Deflection Mode

The second derivative of the deflection goes from negative to positive at the midpoint, thus there is no bending moment present at this location. Since there is no bending moment, the flexure can be split at the midpoint and analyzed as two cantilevered beams with equal and opposite end loads. Half the flexure will then be modeled as a cantilevered beam, as shown in figure 32.

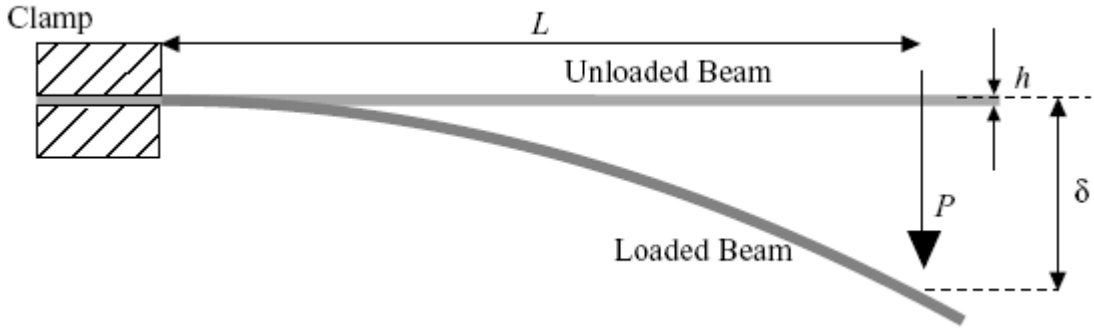

Figure 32: Flexure Simplification

The length L is only half of the total flexure length and δ being only half the displacement of the wall. The deflection at the tip of a cantilevered beam is:

$$\delta = \frac{PL^3}{3EI} \tag{39}$$

In this case, the wall displacement is a known quantity from the differences in expansion rates of the molds and steel structures. The molds will expand by 15.6mm while the steel will only expand by about 4mm. Therefore, an 11.6 mm change in length will be assumed between the steel truss and tip of the mold; with the expansion amount linearly decreasing towards the mold centerline. With the deflection set, there are four unknowns to solve for. The flexure should operate in the elastic deformation region and therefore the yield strain must be accounted for. Since the end deflection is know, the strain in the beam is also known everywhere. The maximum allowable strain in the beam will be set equal to the yield strain (ϵ_{max}).

$$\epsilon_{max} = \frac{\sigma_{max}}{E} \tag{40}$$

Using the standard beam theory:

$$\epsilon_{max} = \frac{M_{max}\, c}{E\, I} \tag{41}$$

where c is half of the flexure thickness, E is Young's Modulus, and I is the moment of interia. From figure 32, the max moment is:

$$M_{max} = P\, L \tag{42}$$

Using equations 40, 41 and 42, equation 39 can be reduced to:

$$\delta_{max} = \frac{\epsilon_{max} * L^2}{3\, c} \tag{43}$$

Notice the maximum allowable deflection is only a function of the material's max strain, flexure length, and flexure thickness. From here two more constraints must be implemented to have a fully constrained design. One constraint could be buckling strength. Assuming that the tooling board is supported by a flexure every 300mm, about

20 flexures will be necessary. Assuming the worst case distributed load of 500 N/m over the 6 meter mold, gives a total load 3000 N. Assuming equal load sharing, each flexure will support 150 N. The buckling load can be determined from Euler Buckling:

$$P_{crit} = \frac{\pi^2 EI}{L^2} \tag{44}$$

To start with, the analysis will be performed to determine the thickness required for a rectangular steel flexure with a 200 GPa Young's Modulus (E), a flexure width (b) of 375mm and a flexure length (L) of 200mm.

$$t_{min} = \sqrt[3]{\frac{12\ P_{crit}\ L^2}{\pi^2 E\ b}} = \sqrt[3]{\frac{12 * 150 * 0.2^2}{\pi^2 * 200 * 10^9 * .375}} \approx\ 0.0007m \tag{45}$$

Thus even for a reasonably long flexure, the required thickness is still fairly small. But this does give a lower bound to the flexure thickness.

Since the intent is to produce these flexures in house, the flexures will be limited to the standard thicknesses of sheet metal and thus gives us finite values for c, but it does not give a full constraint.

Looking back to equation 43, ideally flexure thickness should be minimized in order to maximize the allowable deflection. The Lab usually stocks sheet metal with thicknesses as small as 1mm, and since the goal is to maximize the allowable deflection, the 1mm thickness will be used since it is thinnest gauge available and should offer ample buckling strength.

To finalize the design, a constraint on length or the strain to failure must be created. The strain to failure will be used as the last constraint for this case since there are only a finite number of materials to choose from, and therefore once a material is chosen there will be

a minimum required flexure length. Ideally, the length of the flexure should be minimized in order to keep buckling resistance as high as possible. From equation 43 it can be seen that to minimize length for a given deflection and thickness, the strain to failure must be maximized.

Now a material must be chosen that gives the highest strain to failure in order to minimize the flexure length. Table 2 shows a list of typical engineering metals and their associated required flexure lengths.

Material	E(Pa)	Sig_max (Pa)	e_max	Thickness (m)	L_req (m)	Flexure Length(m)
1018	2.00E+11	2.20E+08	1.10E-03	0.001	0.126	0.252
1020	2.00E+11	3.45E+08	1.73E-03	0.001	0.100	0.201
4130	2.05E+11	4.60E+08	2.24E-03	0.001	0.088	0.176
2024 t3	7.30E+10	2.90E+08	3.97E-03	0.001	0.066	0.132
3003	6.90E+10	1.35E+08	1.96E-03	0.001	0.094	0.189
5052	7.00E+10	1.93E+08	2.76E-03	0.001	0.079	0.159
6AL-4V	1.14E+11	8.80E+08	7.73E-03	0.001	0.047	0.095
303	2.00E+11	2.15E+08	1.08E-03	0.001	0.127	0.254

Table 2: Materials and Required Flexure Length

From the table, the titanium alloy 6Al-4V would allow for the smallest flexure length since it has the highest strain to failure but would be quite expensive and, for this application, the cost cannot be justified. The next best would be the aluminum alloys 2024, 5052, 3003 but once again they are fairly expensive for this application.

As a reasonable compromise, the flexures will be made from 4130 where the high strain to failure is needed and 1018 where the flexures are under a lower strain. Since the wing molds have the wing dihedral built into them, the flexures will either get taller or shorter as needed to continue to support the mold past the dihedral. The minimum flexure height

can be determined for any point along the mold, and from there it can be determine where 4130 is needed and where 1018 can be used instead.

One parameter that is still open is the flexure width. Since the flexures must be attached to the support structure, their width should be great enough to be easily attached to the truss but not protrude past the molds, therefore the flexure width will be set to 375mm, which is the same width of the truss. Figure 33 shows the final configuration of the mold assembly with the flexures.

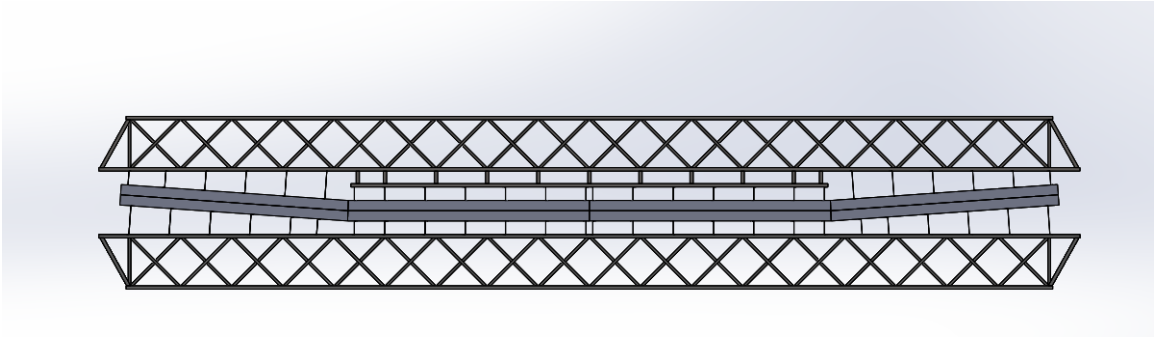

Figure 33: Final Mold Assembly

Figure 34 shows the solid model of the flexure design which is to be cut with a waterjet cutter from flat sheet metal and then bent into the final shape.

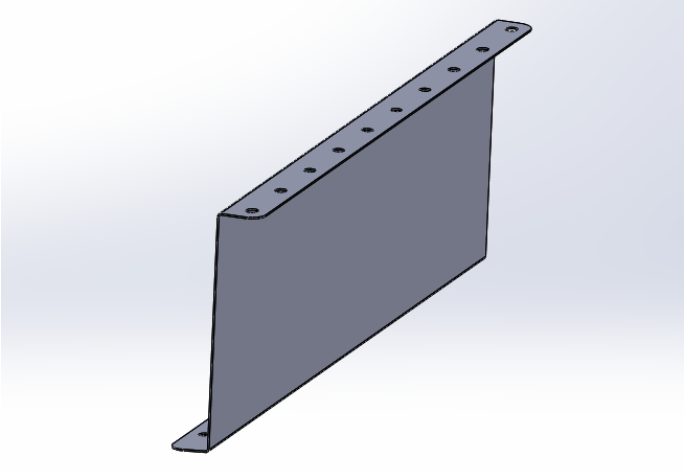

Figure 34 : Final Flexure Design

4.4 Trailing Edge Insert Design

At this point, a solid approach for the wing mold design and support structure has been created. The final pieces needed to produce a wing are the trailing edge inserts. Once again, the difference in expansions will be used to begin the design and from previous calculations the mold expansion is known to be on the order of 15.6mm at the mold tips and the same length of aluminum would be 8.5mm. For the inserts, it would be nearly impossible to produce a single piece trail edge insert. Therefore a large number of inserts will be of a reasonable scale. By making the inserts in sections, the inserts will be able to move with the mold as it expands but as a result small gaps are expected to open up between the inserts as the mold expands. If an acceptable gap distance (γ) is determined then the length of the insert can be determined. From previous experience it was decided that a 0.3mm gap was acceptable and would not allow fibers to move into the gaps, though a small amount of resin could flow into the gap, which would be of little consequence.

The total difference in expansion between the aluminum and tooling board (δ) is about 7mm over a 3 meter free length. Taking the expansion difference and dividing it by the allowable gap gives the number of inserts required (NR) to maintain the maximum gap during expansion. For this design:

$$NR = \frac{\delta}{\gamma} = \frac{7mm}{0.3mm} \approx 24\ inserts \tag{46}$$

But the 24 inserts are only for one side of the mold, therefore the entire assembly will require 48 inserts. Now taking the 3 meter length and dividing it by the number of inserts will give the insert length.

$$L_{insert} = \frac{L}{NR} = \frac{3}{24} = 125mm \tag{47}$$

Since the inserts will be fairly small in size, the inserts can be machined in house on the Haas VF-2 CNC mill. Additionally, since there will be a large number of inserts to make, a jig to hold multiple inserts at a time will increase productivity.

Now that the design and analysis on the mold and supporting structure is complete the process of building the assembly can begin.

4.5 Manufacturing of the Mold Support Structure

The first step in creating the molds is building the truss structures since everything will be attached to them. Each truss is built one side at a time and all attempts are made to keep the rails as straight as possible but since it is welded, some amount or warpage is essentially unavoidable. Figure 35 shows the layout of one side of the support truss before welding.

Figure 35: Support Truss Layout

After the two rails have been welded, jigs are used to align the two sides, then the two trusses are triangulated together with more tubes. Figure 36 shows the truss structure after the two sides have been joined and the finish welding is being done.

Figure 36: Finish Welding Support Truss

The truss is now finished and work on the support flexures can begin. From the CAD model, the different flexures have flat patterns generated in order to be waterjet cut. Once the patterns have been created, the material is gathered and the flexures are cut out of their required material. After all of the flexures have been cut out, a press break is used to bend the flexures into the shape.

Once all of the flexures have been made, they are bolted to the support truss and ready for the molds to be attached. Since bonding to metal can be somewhat challenging, strips of hardwood are screwed to the top of the flexure in order to provide a better surface to bond the molds to. Proset 176/276 epoxy adhesive is then applied to the wood on the flexures and to the bottom of the tooling board. The tooling board pieces are then placed on to the flexures and the adhesive is allowed to cure. Figure 37 shows the completed mold structure.

Figure 37: Finished Mold Half

This process is then repeated for the other mold and then the two mold halves are ready to be machined.

4.6 Mold Machining

One of the molds is then placed in the Lehigh Composites Lab's Hendrick 5-axis router to begin machining of the mold cavity. Since the molds are quite large and extend beyond the travel limits of the machine, only half of the mold can be machined at a time and then it must be flipped around to machine the other half. As a result, care had to be taken to insure that the molds were placed exactly where they needed to be so that the mold cavity is continuous and smooth.

Figure 38 shows one of the molds placed on the router and ready for machining.

Figure 38: Mold Setup for Machining

The mold geometry is then brought into MasterCAM to generate the tool paths for the mold. All surfaces on the mold are machined since the tooling board is not guaranteed to be flat once it was bonded to the flexures. All mating surfaces need to be machined since it reduces any chances of the molds not fitting together properly. Figure 39 shows the machining in progress.

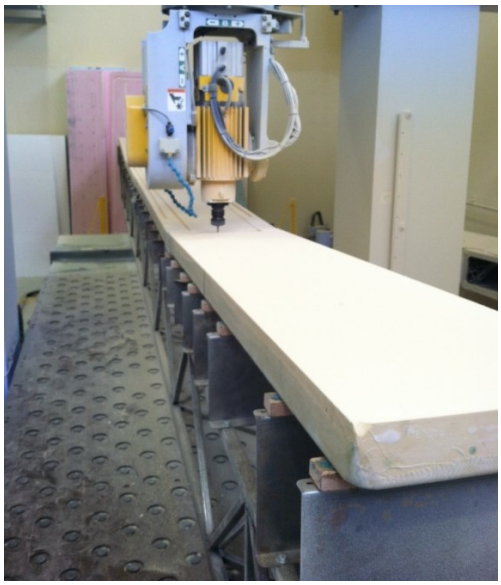

Figure 39: Wing Mold Machining

After the one side is finished being machined, the mold is flipped around and machining continues. Figure 40 shows the final machined mold.

Figure 40: Finished Wing Mold

This process is then repeated for the other mold half, then both molds are ready for sealing, sanding, and release coating.

Since the mold material is quite soft, mold surfaces can easily be abraded away, it was decided to seal the mold surface with epoxy to provide a hard surface which can be sanded with lower risk of distorting the machined profile. An epoxy resin is mixed with a colored talc power and then spread onto the mold surface to seal the mold. The colored talc gives the epoxy some color which makes it easier to see where the mold is sealed, and where it is not. After the epoxy is spread onto the mold, as much resin as possible is wiped off to help keep the coating thin, though the mold surface is porous enough that a fair amount of resin is taken up by the mold initially. A few coats of resin are put on until the surface does not take up any additional resin. The surface is then sanded to a smooth finish and a release agent is applied. The release agent is necessary to allow the finished wing to be easily removed without damaging the mold.

4.7 Insert Machining

Now that the molds are finished and ready for the layup, work can move to the 48 trailing edge inserts that need to be machined. A jig was created to hold 8 inserts at a time for machining. Figure 41 shows the layout for the machining jig.

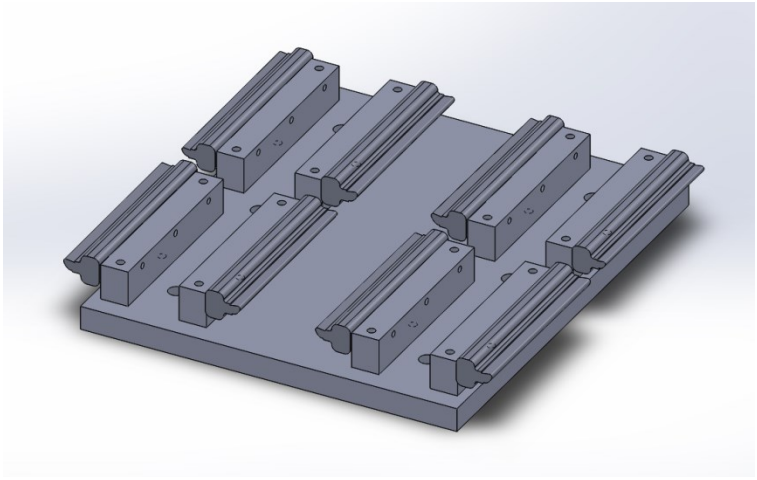

Figure 41: Trailing Edge Insert Jig

Each inserts has two alignment holes drilled and reamed in the back to allow for each insert to be flipped over and located properly using dowel pins in the jig. Additionally, there is one tapped hole in the center which is used to hold the inserts firmly against the jig. Figure 42 shows all of the machined inserts after they were sanded and mold released.

Figure 42: Finished Trailing Edge Inserts

Finally before the layup can begin, the foam molds for the webs must be cut out. Using a hotwire and templates, the foam molds are cut from blocks of polystyrene. The foam molds are then put inside the lay flat tubing and placed under vacuum. At this point, all of the supplies necessary for the layup are prepared and ready to go.

5 Wing Construction

The first step in the process is cutting all of the plies for the entire layup. Metal templates were laser cut for all of the skin plies to ensure the proper sizing and fitment of each piece. Just for the wing skins, there are 96 different plies that are split between the two mold halves. The spar flange's 36 plies are then cut along with the 144 web plies. Once all of the plies are cut, the layup process can begin. In order to help ensure consistent manufacturing, a layup procedure was created and is given in Appendix D.

5.1 Wing Layup

To begin, thin strips of unidirectional carbon are laid spanwise along the leading edge on both mold halves. This is to provide a little extra material at the joint of the two molds and helps create a better leading edge. After the leading edge pieces are laid, the first +45° plies are laid along the wing as show in figure 43.

Figure 43: Laying of 1st Wing Skin Ply

After the first ply of the wing skin is laid down, the ply is debulked for 30 minutes while the same procedure is done on the other mold half. Figure 44 shows one mold under vacuum being debulked, while the other mold is having the wing skin laid down.

Figure 44: Debulking Fist Ply and Continuing Layup

This process is then repeated for the -45° skin plies on both molds. After the first two skin plies are laid, the spar flanges are laid onto the mold. Figure 45 shows the spar flanges being laid on top of the first two skin plies.

Figure 45: Laying of Wing Spar Plies

The spar is debulked for 15 minutes after every 3 plies to help ensure low porosity in the final part. Once the 18 plies for each spar flange have been laid and debulked, the second -45° and +45° plies can be laid and then debulked. Once the second set of skin plies have been debulked, the wing skin is complete and now work on the internal webs can begin. The three foam molds, still under vacuum in their lay-flat tubing, are placed onto the mold. Templates are used to locate the foam molds along the entire length of the wing. Figure 46 shows the placement of the foam form while the first web plies are being laid.

Figure 46: Laying Web Plies over Foam Molds

Once the foam molds are in place, the web plies are laid over the top of the foam molds, which helps secure the foam mold in place as well. These plies are then debulked to help ensure a compact laminate as well as help fix the foam molds in place further. Care must be taken that the foam molds are not deformed during this process, since their size is critical in ensuring the webs contact both sides of the mold.

After the web plies have been laid, the trailing edge insert plies are placed followed by the trailing edge inserts. The trailing edge plies are then wrapped around the inserts and

debulked to ensure the plies conform to the foam molds. After the trailing edge plies have been debulked, more spanwise strips of unidirectional carbon fiber are placed at all the joints to ensure low porosity and a strong joint. Finally, four lay-flat tubes are placed in the "valleys" between the foam molds (sections 1, 3, 5 and 7).

The layup is now complete and the molds are ready to be closed. Due to the size of the molds an overhead crane was used to lift up the bottom skin mold and then gently placed on to the top skin mold. Figure 47 shows this in progress while also ensuring plies do not make their way on to the mating surfaces of the molds.

Figure 47: Closing the Wing Mold

The wing is then placed in the oven and cured at 85 degrees C for a minimum of 12 hours. The decision to go with the fairly low cure temperature was to lower the thermal expansion of the molds slightly in hopes of minimizing the negative effects of the CTE mismatch between the carbon fiber and tooling board. Thermocouples were placed in the lay-flat tubes throughout the wing in order to monitor the wing's temperature throughout

the curing process rather than relying on the oven's air temperature alone. With the use of the thermocouples, it could be guaranteed that the wing was fully cured before removing it from the oven.

Once removed from the oven, the molds are separated and the wing can be removed with the trailing edge inserts still attached. The inserts are then removed individually from the wing and the part is complete. Figure 48 shows a finished wing.

Figure 48: Finished Wing

5.2 Wing Structural Testing

The finished wing was then given a simple proof load to prove the structural integrity of the wing. Figure 49 shows this test in progress.

Figure 49: Preliminary Wing Testing

To further test the wing's structural integrity, a 3.5kN distributed load was placed along the wing while the wing was only being supported at the center. While this load is nowhere near failure load, it was deemed sufficient to allow for preliminary test flights of the JetStreamer. Figure 50 shows this test in progress.

Figure 50: 3.5 KN Proof Load of Wing

The wing showed no signs of damage during the test and gave off no major acoustical events either, which are often a sign of damage initiation in composites.

Prior to any load test, the wing did show some surface imperfections on the wings skin. These are believed to be an effect of the mold's relatively high CTE and the carbon fiber's approximately zero CTE. Some larger test pieces were made on the full size molds to help determine ways to reduce these surface imperfections. Figure 51 shows a test section made with the same process as the previous wing.

Figure 51: Typical Wing Skin Defects

Most of the defects run spanwise along the wing, these defects also line up perfectly with the joints between the wing skin and webs, which were seen to some degree in earlier tests. This is once again somewhat expected since the joint makes it very difficult for the vacuum bags to apply force in those areas. In the future, extra material will be put in the

joints to make the joint larger and therefore easier for the vacuum bag to apply force to the joint.

The fibers along the defects do not seem to be dry or show signs of delamination; because of this, the imperfections are believed to be mainly cosmetic and can be fixed with filler and paint without any major concern. Tests were also performed by adding plies in the chord direction to give the ply more support but appeared to have minimal effects on the size of the imperfections.

With these corrections in mind, four more wings were constructed, each showing similar skin imperfections but improvements were made with each wing. Once all the processing materials (vacuum bags, foam molds, etc) were removed from the inside of the wing, the wing weighed in at a mere 7.5 kg.

5.3 Conclusions of Wing Manufacturing

The tooling board wing molds with aluminum trailing edge inserts were straight-forward to machine. The polystyrene foam molds worked quite well for the six internal webs. The wing manufacturing is considered a major success. While there were surface imperfections, they are believed to be of no major structural importance.

6 Wing Control Surfaces

Now that multiple wings have been produced, attention must shift to the other parts of the aircraft. The next parts tackled were the flaps and alierons.

6.1 Initial design

From the earlier designs, a control surface profile is set, but there is no design for the actual structure of it. In efforts to continue developing one-shot processes for the aircraft's components, carbon fiber prepreg is again a clear choice. To begin a hollow control surface will be designed.

For each wing, there will be 4 different control surfaces which are comprised of two ailerons and two flaps with lengths of 1.8m and 1.2m respectively. The main concern with control surfaces is flutter which is heavily dependent of torsional stiffness as well as the control surface center of gravity. For approximate analysis, control surfaces will be modeled as a non-circular constant cross-section tubes. The reference cross-section used will be that of the middle of the control surface. From the CAD model, cross-section properties of the middle sections are:

$$A_{flap} = 7.004\ cm^2 \quad U_{flap} = 18.04\ cm \qquad A_{aileron} = 3.23\ cm^2 \quad U_{flap} = 12.87\ cm$$

The torsional stiffness can be computed for each control surface by, once again using:

$$\theta = \frac{T\ L\ U}{4\ GA^2\ t} \tag{48}$$

As a starting point, the control surface will have 3 plies of unidirectional carbon oriented [+45,-45,+45]. This laminate is symmetric but not balanced. Using Mathematica to perform the tensor transformations due to the laminate being non-balanced, a shear modulus (G) of 28.6 GPa is calculated. Using a laminate thickness of 0.6 mm and the properties from above, the approximate torsional stiffness for the control surfaces are:

$$\left(\frac{T}{\theta}\right)_{Flap} \approx 103\ \frac{Nm}{deg} \quad \left(\frac{T}{\theta}\right)_{Aileron} \approx 46\frac{Nm}{deg} \tag{49}$$

As before, this is a worst case loading since, in reality, the moment will be distributed along the control surface and the effective length can change depending on control horn placement. These calculations serve to show if the structure is greatly over-built, or under-built. Looking at the hinge moment coefficient formula:

$$C_{hm} = \frac{M_h}{\frac{1}{2}\rho\ v^2\ S_c\ c_c} \tag{50}$$

Where M_h is the hinge moment, ρ is air density, v is velocity, S_c is control surface area, and c_c is the control surface chord length. For the control surface chord, it was chosen to be 22% of the airfoil chord length; this value was chosen because it has been used in production aircraft with great success and gives sufficient control effectiveness. The hinge moment coefficient can be approximated as [4]:

$$C_{hm} = -C_l\left(\frac{\partial C_h}{\partial C_l}\right) - \delta\left(\frac{\partial C_h}{\partial \delta}\right) \tag{51}$$

Where δ is control surface deflection in radians. Using the 22% control surface chord $\frac{\partial C_h}{\partial C_l}$ can be approximated as 0.1 while $\frac{\partial C_h}{\partial \delta}$ is approximately 0.62. As a worst case loading, it will be assumed the control surface is deflected the maximum of 30 degrees.

The hinge moment is a function of velocity and the Coefficient of lift. From the V-n diagram, a relationship between the velocity and maximum coefficient of lift allowed by the structure can be determined. Then taking the maximum coefficient of lift vs. velocity relation and putting it into the hinge moment equation, a relationship between the maximum hinge moment and velocity can be created. A plot of this function is shown in figure 52.

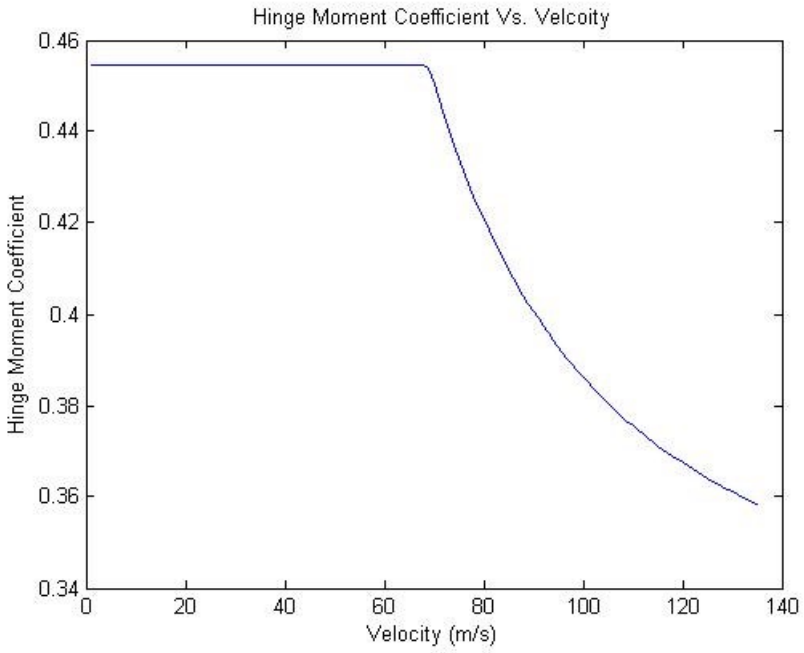

Figure 52: Hinge Moment Coefficient vs. Velocity

Now the hinge moment can be made to be only a function of velocity by using the C_{hm} vs. velocity relation to give a maximum hinge moment for a given velocity. This equation has the following form:

$$M_{hinge} = C_{hm}\left(\frac{1}{2}\rho v^2 b_{control} c_{control}^2\right) \tag{52}$$

Using the previous relations, a MATLAB script was created to calculate the hinge moment for a flap with a chord ($c_{control}$) of 74mm and a length ($b_{control}$) of 1.8m. Plotting the moment as a function of velocity is given in figure 53.

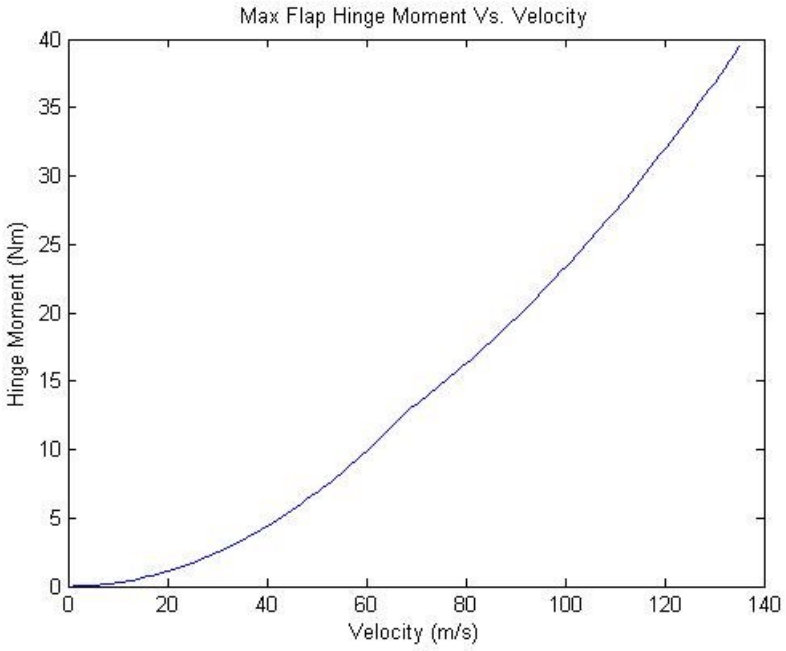

Figure 53: Maximum Flap Hinge Moment vs. Velocity

From figure 53, the max hinge moment is shown to be approximately 40 Nm. Looking back to the control surface torsional stiffness, the flaps will have fairly little deflection from the hinge moment when compared to the maximum deflection of the flap. Once

again, keeping in mind that the hinge moment will be distributed along the length whereas the stiffness calculation assumes the moment is applied to the end of the control surface, so even lower deflections would be expected.

Repeating the calculations for the ailerons gives a hinge moment of about 15 Nm. As before, the hinge moment will cause only a small deflection of the control surface. Therefore original layup schedule is appropriate for both the flaps and ailerons. While the layup is considered to be sufficient, care must be taken in the future to ensure the control surfaces are mass balanced around the hinge in order to reduce the risk of flutter.

6.2 Flap Prototype

Designs have been created for the flaps and ailerons and are now ready to be manufactured. Since the control surfaces will be built in four sections the molds are much smaller than the full wing mold, and as a result the use of aluminum as a mold material becomes much more cost effective and makes the molds easier to produce. While the flap and aileron molds are too long to machine in one piece on a HAAS VF-2, the molds can be machined in multiple sections and assembled into a larger mold. As usual though, a small test mold will be made to verify the intended process and produce initial prototypes.

After the test molds were finished being machined, the molds were sanded, polished, and mold released. The layup for the control surfaces is fairly simple, but just as with the large wings, thin strips of unidirection fiber are run along the leading edge joints on both

the top and bottom molds to ensure a defect free leading edge. The first +45°ply is then laid down on the mold as shown in figure 54.

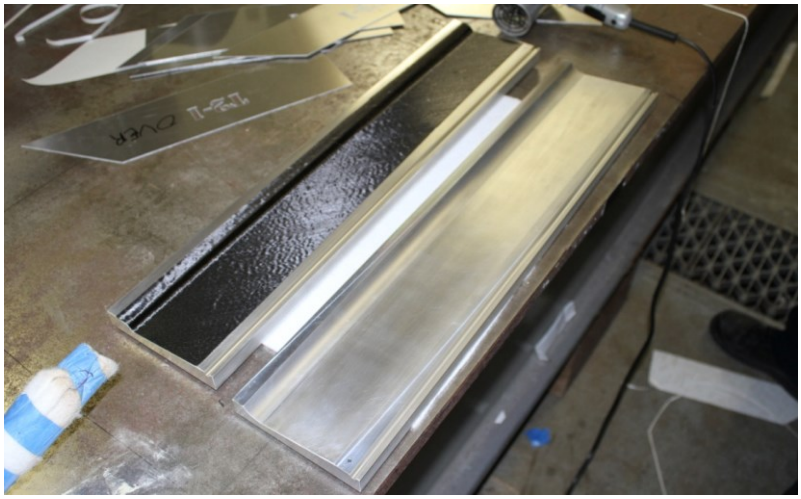

Figure 54: 1st Ply of Flap Layup

Once the first plies are laid on both molds, the plies are debulked in order to produce a defect free surface. Figure 55 shows both molds being debulked.

Figure 55: Flap Ply Debulking

After debulking the -45° and +45° plies are laid down. Finally, more thin strips of fibers are places along the trailing edge to ensure the top and bottom skins are bonded well at the trailing edge joint. Peel ply is then run along both skins in order to aid in air evacuation under vacuum. Figure 56 shows the peel ply in place as well as the trailing edge fibers in position.

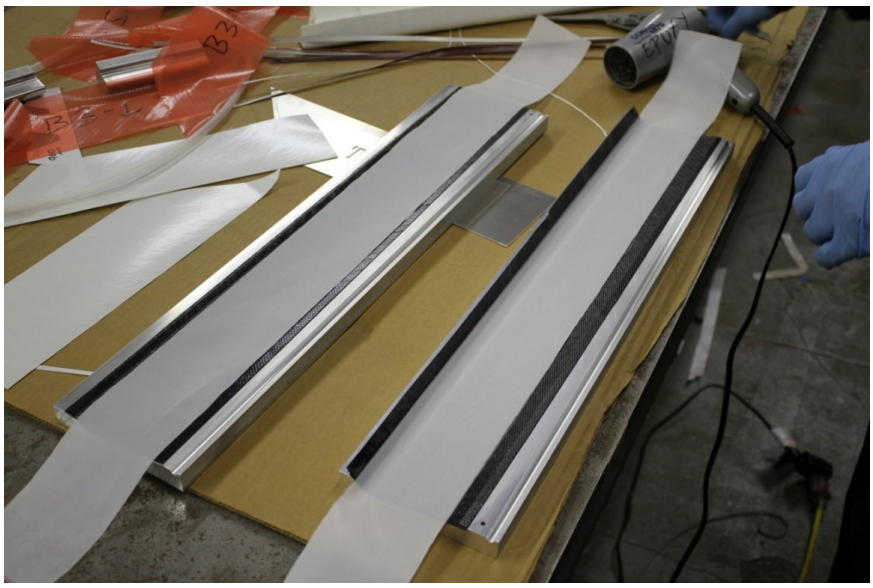

Figure 56: Layup Finished and Ready to Close Molds

The molds are then closed and placed under vacuum. The part is then cured at 120°C for 3 hours and a finished flap is ready to be removed from the mold once cooled. Figure 57 shows the finished part when removed from the mold.

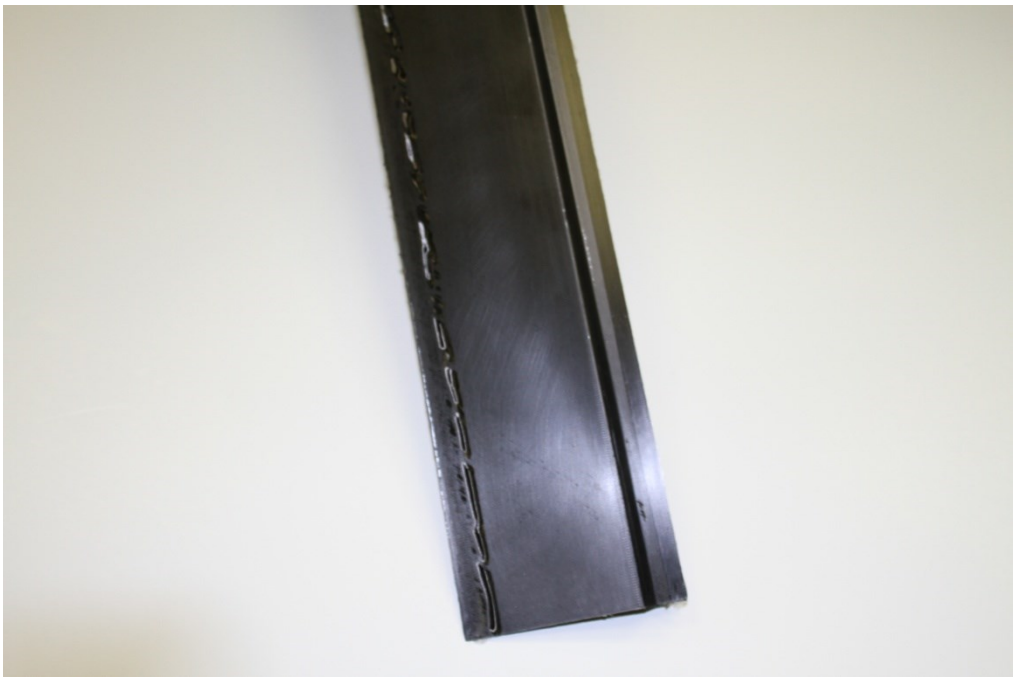

Figure 57: Finished Flap Prototype

The finished part showed good surface finish everywhere except at the trailing edge, where there are some skin wrinkles. This is caused by the vacuum bag not being able to work itself into the corner while curing and possibly not enough fiber in the trailing edge. As a result, the successive control sufaces had an increased number of fiber strips added along the trailing edge, as well as the vacuum bag placed as close to the trailing edge as reasonably possible. Figure 58 shows the results of the later tests which show an almost defect free surface along the trailing edge.

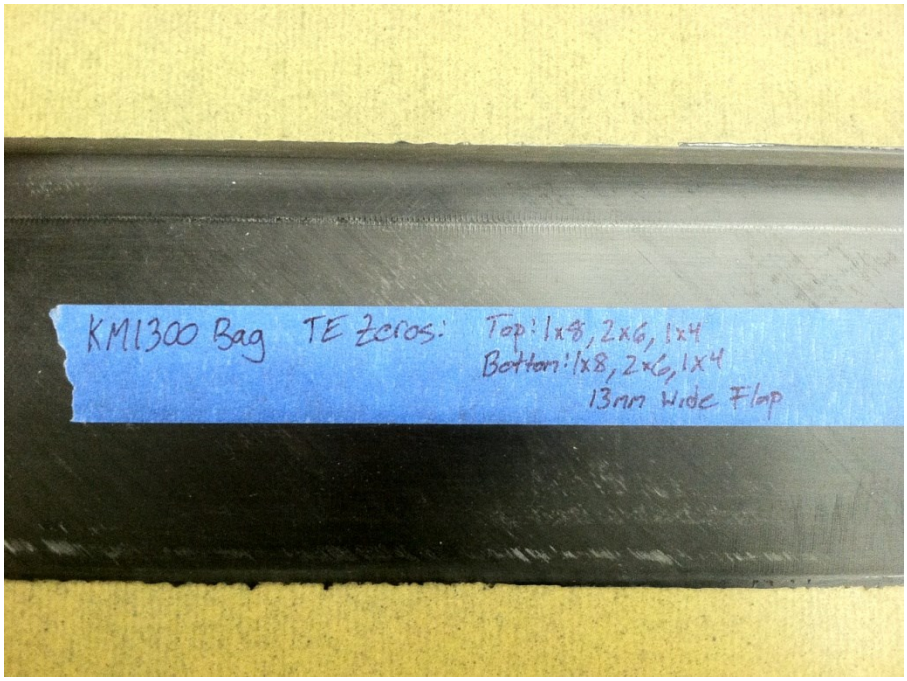

Figure 58: Improved Flap

The tests showed that good quality flaps and ailerons could be manufactured using this technique.

6.3 Wing Test Section

Before continuing on, a test wing section was constructed using the earlier wing test sections along with the recent flap test section. These parts allowed a fully functioning section of the wing to be created. Hinges and a control horn were attached to the flap and then the assembly was attached to the wing section. A servo was fitted into the main wing and attached to the aileron control horn. Figure 59 shows the working wing section.

Figure 59: Functional Wing Section

The test wing section showed the system operates as intended and that construction can continue with confidence in a final working product.

6.4 Flap and Aileron Manufacturing

To produce all of the control surfaces for the JetStreamer, the first step was creating the molds for all of the control surfaces; this was done by machining the molds in smaller sections and attaching them to a box beam as a support structure. Since both the molds and box beams were made of aluminum, there would be no CTE mismatch problems. Figure 60 shows the completed molds after sanding and polishing.

Figure 60: Finished Flap Molds

The layup procedure for both the flaps and ailerons was the exact same as the test parts. The manufacturing of the flaps and ailerons went very smoothly and gave consistent results similarly to the test flap. Figure 61 shows the typical surface finish for the control surfaces.

Figure 61: Typical Control Surface Finish

At this point all of the control surfaces have been made and a fully functional wing can now be assembled. At the time of writing this paper, the project has just reached this stage.

7 Future Work

While a substantial amount of progress has been made on building a functioning dynamic soaring UAV, there is still considerable work that must be done. Some of the large tasks that must be done before the JetStreamer is ready for flight testing are fitting the control surfaces to the wings, the design and manufacturing of a horizontal stabilizer, and design and manufacturing of the fuselage and vertical stabilizer.

7.1 Control Surface Fitting

While the control surfaces are complete, they must still be installed on the wings and checked for proper alignment and function. Care will have to be taken when installing the hinges to ensure they do not bind throughout their travel as well as have the desired angular deflections. Control horns will also need to be attached to the control surfaces to allow for an actuator to be fitted to them. Once the control surfaces have been installed on the wing, they will be hooked up to servos that have been installed in the wing. After the servos have been attached, the wing will be a fully functional system.

7.2 Horizontal Stabilizer

A horizontal stabilizer must be designed and manufactured for the airplane. The horizontal stabilizer will be built in a similar manner to the main wing but with a flexure, rather than a hinge, between the horizontal stabilizer and the elevator. Both will be produced together in a single cure.

7.3 Fuselage and Vertical Stabilizer

Finally the fuselage and vertical stabilizer must be built. These are presently being designed.

References

[1] C. D. Cone, "A Mathematical Analysis of the Dynaimc Foaring Flight of the ALbatross with Ecological Interpretations," Virginia Intitute of Marine Science, 1964.

[2] J. L. Grenestet, "On Dynamic Soaring," Lehigh Dept. of Mechanical Engineering, 2010.

[3] J. D. Anderson, Fundametals of Aerodynamics, McGraw-Hill.

[4] I. H. Abbot and A. E. v. Doenhoff, Theory of WIng Sections, Dover, 1959.

[5] J. D. Anderson, Aircraft Performance, WCB/McGraw-Hill, 1999.

A Airfoil Coordinates

Ridder-JLG-flatback

1	0
0.99637	0.000658274
0.99031	0.001757212
0.98349	0.002993969
0.97596	0.00435948
0.96791	0.00581929
0.95946	0.007351636
0.95065	0.008949266
0.94158	0.010594045
0.93234	0.012269652
0.923	0.013963394
0.91358	0.015671643
0.90413	0.017385332
0.89468	0.019099022
0.88521	0.020816338
0.87573	0.022535467
0.86624	0.02425641
0.85672	0.025982794
0.8472	0.027709177
0.83767	0.029437373
0.82814	0.03116557
0.81858	0.032899207
0.80901	0.034634658
0.7994	0.036377362
0.78977	0.038123693
0.78011	0.039875464
0.77043	0.041630862
0.76073	0.043389887
0.75102	0.045150725
0.74128	0.046917004
0.73153	0.048685096
0.72173	0.050462255
0.71187	0.052250295
0.70197	0.054045589
0.69202	0.055849949
0.68203	0.057661564
0.67205	0.059471365
0.66209	0.061277539
0.6522	0.063071019
0.64237	0.064853618
0.63262	0.066621711
0.62296	0.068373482
0.61338	0.070110746
0.60387	0.071835315
0.59442	0.073549005
0.58504	0.07525
0.57569	0.07693
0.56636	0.07852
0.55704	0.08002
0.54771	0.08145
0.53835	0.08281
0.52897	0.0841
0.51957	0.08532
0.51014	0.08647
0.50069	0.08755
0.49123	0.08856
0.48175	0.08951
0.47225	0.09039
0.46274	0.09121
0.45322	0.09195
0.4437	0.09264
0.43417	0.09325
0.42464	0.09379
0.41511	0.09427
0.40557	0.09468
0.39603	0.09503
0.38648	0.09531
0.37693	0.09553
0.36738	0.09569
0.35783	0.09578
0.34829	0.09581
0.33876	0.09576
0.32926	0.09566
0.31978	0.09547
0.31031	0.09523
0.30087	0.09492
0.29144	0.09453
0.28205	0.09409
0.27269	0.09357
0.26337	0.09297
0.25408	0.0923
0.24485	0.09156
0.23565	0.09075
0.22651	0.08985
0.21742	0.08888
0.20839	0.08782
0.19942	0.08668
0.19053	0.08547
0.1817	0.08416
0.17295	0.08277
0.16429	0.0813
0.15572	0.07972
0.14726	0.07807
0.13892	0.07633
0.13071	0.07449
0.12264	0.07256
0.11473	0.07053
0.10699	0.06842
0.09944	0.06623

0.09209	0.06395
0.08498	0.0616
0.07812	0.0592
0.07155	0.05673
0.0653	0.05424
0.05938	0.05173
0.05383	0.04922
0.04865	0.04674
0.04384	0.04429
0.03942	0.04189
0.03536	0.03955
0.03166	0.03728
0.02828	0.0351
0.02522	0.03299
0.02244	0.03097
0.01991	0.02902
0.01762	0.02715
0.01554	0.02535
0.01365	0.02361
0.01194	0.02194
0.01039	0.02032
0.00898	0.01876
0.0077	0.01725
0.00654	0.01578
0.0055	0.01436
0.00456	0.01299
0.00372	0.01165
0.00298	0.01026
0.00232	0.00885
0.00175	0.00765
0.00126	0.00667
0.00086	0.00553
0.00053	0.004
0.00028	0.00235
0.00011	0.00097
0.00002	0.00015
0.00001	-0.00004
0.00001	-0.00004
0.00008	-0.00062
0.00025	-0.00189
0.00055	-0.00363
0.00097	-0.00506
0.00152	-0.0059
0.00219	-0.00673
0.00298	-0.0078
0.00389	-0.00879
0.00493	-0.00963
0.00609	-0.01044
0.00737	-0.01122
0.00875	-0.01192
0.01025	-0.01258
0.01187	-0.01322
0.01362	-0.01383
0.01551	-0.01443
0.01755	-0.01502
0.01976	-0.01561
0.02218	-0.0162
0.02483	-0.01679
0.02774	-0.0174
0.03095	-0.01801
0.03452	-0.01864
0.03851	-0.0193
0.04297	-0.01997
0.04797	-0.02066
0.05357	-0.02137
0.05981	-0.02211
0.0667	-0.02285
0.07423	-0.02361
0.08232	-0.02436
0.09089	-0.0251
0.09984	-0.02581
0.10908	-0.0265
0.11854	-0.02715
0.12815	-0.02777
0.13787	-0.02837
0.14767	-0.02891
0.15754	-0.02945
0.16745	-0.02993
0.17739	-0.0304
0.18737	-0.03083
0.19737	-0.03123
0.20739	-0.0316
0.21743	-0.03195
0.22747	-0.03228
0.23752	-0.03257
0.24757	-0.03285
0.25762	-0.0331
0.26768	-0.03333
0.27775	-0.03353
0.28782	-0.0337
0.29789	-0.03384
0.30795	-0.03396
0.31802	-0.03406
0.32809	-0.03414
0.33816	-0.03418
0.34824	-0.03419
0.35833	-0.03418
0.3684	-0.03415
0.37848	-0.03409
0.38855	-0.034
0.39864	-0.03388
0.40874	-0.03374
0.41885	-0.03356
0.42896	-0.03335
0.43906	-0.03313
0.44917	-0.03288

0.45927	-0.03261
0.46938	-0.03231
0.47949	-0.03198
0.48963	-0.03161
0.49978	-0.03123
0.50995	-0.03082
0.52014	-0.03038
0.53032	-0.02992
0.54051	-0.02944
0.55069	-0.02896
0.56088	-0.02844
0.57108	-0.02791
0.58129	-0.02735
0.59152	-0.02677
0.60177	-0.02617
0.61202	-0.02555
0.62228	-0.02493
0.63252	-0.02429
0.64277	-0.02364
0.65303	-0.022961036
0.6633	-0.02228141
0.67359	-0.02160046
0.68387	-0.020920172
0.69416	-0.020239223
0.70445	-0.019558273
0.71475	-0.018876662
0.72505	-0.018195051
0.73537	-0.017512116
0.7457	-0.016828519
0.75604	-0.016144261
0.7664	-0.015458679
0.77675	-0.014773759
0.78711	-0.014088177
0.79745	-0.013403919
0.80777	-0.012720984
0.81808	-0.012038711
0.82837	-0.011357762
0.83865	-0.010677474
0.8489	-0.009999171
0.85914	-0.009321531
0.86935	-0.008645875
0.87955	-0.007970882
0.88971	-0.007298535
0.89985	-0.006627512
0.90996	-0.005958474
0.92001	-0.005293406
0.92996	-0.004634957
0.93977	-0.003985772
0.94936	-0.003351145
0.95863	-0.002737695
0.96748	-0.002152039
0.97578	-0.001602779
0.98341	-0.001097857
0.99027	-0.000643891
0.99636	-0.00024088
1	0

B MATLAB Aircraft Performance Code

```
% Jacob Patterson
% Dynamic Soaring UAV

clear
clc

%Constants
rho = 1.23 %STP density kg/m^3
u = 1.82e-5 %Viscosity of air STP
g = 9.81 %Gravity

%Estimated Airplane Characteristics
w = 50; %kg
m = w
b = 6.5 %Wing Span (m)
cr = .375 %Root Chord Length
tr = .5 %Wing Taper Ratio
ct = cr*tr %Tip Chord Length

P = 2200 %Engine Power in Watts

e = .8; %Oswald Effeciency
pn = .8; %Propeller Effeciency
en = .8 ;%Electric motor Effeciency

%Control Surfaces
Vht = .7;%Horizontal Tail Volume Ratio
Vvt = .04; %Vertical Tail Volume Ratio
lht = 24*.0254; %Horizontal Tail Distance from C.G.
lvt = 24*.0254; %Vertical Tail distance from C.G.
ARht = 3;
ARvt = 2;

%Conversions
S = (cr+ct)/2*b %Surface Area
L = w*g; %Lift force in N
%c1 = cr; %Root Chord Lenght
%c2 = (cr-ct)/(b/2); %Wing Tip Chord Length
MAC = 2*(cr^2+cr*ct+ct^2)/(3*(cr+ct)) %Mean Chord Length
c = MAC; %Chord Length
wl = w*10/S; %Wingloading in g/dm^2
wcl = w*1000/(S*100)^1.5
AR = b/MAC %Aspect Ratio

%Airfoil Characteristics
Cdo = .008;
Clmax = 1.3;
dcda = .11;
zlAoA = -3;
```

```
%Other Assumptions
Cd_body = .05; %Streamlined fuselage
A_f = pi*.09^2; %Fuselage with a 180mm diameter frontal area

%Calculations
Pa = P*pn*en
theostallspeed = sqrt(2/rho*L/S*1/Clmax)
%VminSink = sqrt(2)*(m*g)^.5/((3*pi*e*f0)^.25*sqrt(b*rho))

Sht = Vht*MAC*S/lht;
Svt = Vvt*b*S/lvt;

bht = sqrt(ARht*Sht)*1000/25.4;
bvt = sqrt(ARvt*Svt)*1000/25.4;

cht = (bht/ARht);
cvt = (bvt/ARvt);

n=0

for i = 10:100
   n = n+1;
   v(n)= i; %Velocity
   q = 1/2*rho*v(n)^2; %dynamic pressure
   l(n) = L %Lift Force
   Cl(n) = L/(S/2*rho*v(n)^2); %Coefficent of Lift
   Cd(n) = Cdo + Cl(n)^2/(pi*e*AR); %Coefficent of Drag
   D(n) = Cd_body*q*A_f + Cdo*q*S + Cl(n)^2/(pi*e*AR)*S*q; %Drag Force
   Cde(n) = D(n)/(S*q) %Effective Cd normalized to wing area
   lod(n) = Cl(n)/Cd(n); %L/D Ratio
   LoD(n) = L/D(n);% L/D Ratio
   Tr(n) = D(n); %Thrust Required
   Pr(n) = Tr(n)*v(n); %Power Required
   AoA(n) = zlAoA + Cl(n)/dcda; %Angle of attack
   ss(n) = theostallspeed; %Stall Speed
   Re(n) = rho*v(n)*c/u; %Reynolds Number
   Vv(n) = (Pa-Pr(n))/(m*g); %Climb rate available;
   %vh = sqrt(2*m*g)/((3*pi*e*f0)^.25*sqrt(b*rho));
end

[Vvmax,index] = max(Vv')
% [minpr,index] = min(Pr);
% Vprmin = v(index);
% [maxLod,index] = max(lod);
% Vlodmax = v(index)

figure(1)
%subplot(3,2,1)
plot(v,LoD)
title('L/D vs. Speed')
xlabel('Velocity (m/s)')
ylabel('L/D')
```

```
figure(2)
%subplot(3,2,3)
plot(v,Tr)
title('Trust Required')
%axis([0 25 0 3])
xlabel('Velocity (m/s)')
ylabel('Thrust Required (N)')

figure(3)
%subplot(3,2,5)
plot(v,Pr,[0 100],[Pa,Pa])
title('Power Required')
legend('Power Required','Power Available','location','NorthWest')
%axis([0 25 0 100])
xlabel('Velocity (m/s)')
ylabel('Power Required (W)')

figure(4)
%subplot(3,2,2)
plot(v,Vv,'b-',[theostallspeed(1) theostallspeed(1)],[-6 4],'m-.')
title('Climb Rate')
axis([0 100 -6 4])
xlabel('Velocity (m/s)')
ylabel('Climb Rate (m/s)')
legend('Max Climb Rate','Stall Speed','location','NorthEast')

figure(5)
%subplot(3,2,4)
plot(v,AoA,v,ss)
title('AoA vs Speed')
axis([0 100 -10 15])
xlabel('Velocity (m/s)')
ylabel('AoA (deg)')

figure(6)
%subplot(3,2,6)
plot(v,Re)
title('Reynolds Number vs Speed')
xlabel('Velocity (m/s)')
ylabel('Reynolds Number')

figure(7)
plot(v,D)
title('Drag vs. Velocity')
xlabel('Velocity (m/s)')
ylabel('Drag (N)')
```

C MATLAB Spar and Web Design

```
%Dynamic Soaring UAV Spar and Web Design
clear
clc

%Constants
g = 9.81

%Design Properties
m = 50 %kg
b = 6.5 %Wingspan
c = .375 %Chord
pt = .125 %Airfoil Percent Thickness

%Load Case
fos = 20 %Factor of Safety
w = fos*m*g/b %beam loading (Assume uniform distributed load
Mmax = .5*w*(b/2)^2 %Max Moment

sigwr = .7e9 %Compression Buckling Stress
TauMax = sigwr/2 %Maximum shear stress for +/-45 laminate

%Beam Calcs
bc = c*pt/2 %Flange Distance from centerline
t = .00015 %Composite Skin thickness

n=0
width = .09
taper = .002
for i = 0:.005:b/2
   n = n+1
   x(n) = i;
   M(n) = .5*w*(b/2-i)^2;
   r(n) = bc - .555*bc*(i/(b/2));
   Ireq = M(n)*r(n)/sigwr;
   Areq(n) = Ireq/(2*r(n)^2);
   A = 0;
   k=0;
   while A<Areq
      k = k+1 ;
      plyA = (width - (k-1)*taper)*t;
      A = A + plyA;
   end
   nreq(n) = k;
   nreq(n) = ceil((Areq(n)/width)/t)

   %Shear Stress Calculations
   V(n) = w*b/2 - w*x(n)
   ta = (width-(k-1)*taper) %Top Width
   tb = width %Base Width
   As = k*t*(ta+tb)/2
```

```
    Cy = k*t*(2*ta+tb)/(3*(ta+tb)) %Centroid location of Trapezoid from base
    Q(n) = As*(r(n) - Cy)
    I(n) = 2*As*(r(n) - Cy)^2
    wt(n) = V(n)*Q(n)/(I(n)*TauMax)


end
z = 0;
for y = 2:n
    diff = nreq(y)-nreq(y-1);
    if diff ~= 0;
        z = z+1;
        pos(z)=2*x(y);
    end
end

figure(1)
plot(x,M)
title('Bending Moment vs. Distance from Centerline')
xlabel('Distance from Centerline (m)')
ylabel('Bending Moment (Nm)')

figure(2)
plot(x,nreq)
title('Plies Required vs. Distance from Centerline')
xlabel('Distance from Centerline (m)')
ylabel('Number of Plies')

figure(3)
plot(x,Areq)
title('Area Required vs. Distance from Centerline')
xlabel('Distance from Centerline (m)')
ylabel('Number of Plies')

figure(4)
plot(x,V)
title('Shear Load vs. Distance from Centerline')
xlabel('Distance from Centerline (m)')
ylabel('Shear Load (N)')

figure(5)
plot(x,wt)
title('Required Web Thickness Vs. Distance from Centerline')
xlabel('Distance from Centerline (m)')
ylabel('Web thickness (m)')
```

D Wing Layup Procedure

1. Prepare molds
    a. Remove remaining epoxy
    b. Repair any damage to surface
    c. clean
    d. Mold Release (chemlease 41-90 EZ)
2. Prepare Trailing Edge inserts
    a. Remove epoxy
    b. Clean
    c. Mold release (NC-770)
3. Prepare Foam Inserts
    a. 24 pieces total (8 per web)
    b. Trim ends short of mold end (250mm cut off each end)
4. Cut Pre-preg
    a. -+/-45 Outer Skins (T01-T48 and B01-B48) (96 pieces total) Use templates
        i. Mark kink in T06,T07,T18,T19,etc.
        ii. Cut+45 with template right side up (T1-12,T37-48, B1-12,B37-48)
        iii. Cut -45's with template upside down (T13-36, B13-36)
    b. Leading Edge Zeros (16 pieces total)
        i. 4pcs 1.8mx8mm
        ii. 4pcs 1.8mx6mm
        iii. 4pcs 1.2mx8mm
        iv. 4pcs 1.2mx6mm
    c. Main spar caps (56 pieces total)-Mark centers. Taper ends as indicated to zero except first and last plies
        i. 2pcs 3.89mx90mm taper 90mm
        ii. 2pcs 3.79mx84mm taper 205mm
        iii. 2pcs 3.788mx88mm taper 88mm
        iv. 2pcs 3.686mx86mm taper 86mm
        v. 2pcs 3.38mx82mm taper 170mm
        vi. 2pcs 3.04mx80mm taper 155mm
        vii. 2pcs 2.73m78mm taper 140mm
        viii. 2pcs 2.45mx76mm taper 130mm
        ix. 2pcs 2.19mx74mm taper 115mm
        x. 2pcs 1.96mx72mm taper 110mm
        xi. 2pcs 1.74mx70mm taper 100mm
        xii. 2pcs 1.54mx68mm taper 95mm

xiii. 2pcs 1.35mx66mm taper 85mm
xiv. 2pcs 1.18mx64mm taper 85mm
xv. 4pcs 1.165mx90mm taper 90mm & taper 540mm→20mm
xvi. 2pcs 1.01x62mm taper 75mm
xvii. 2pcs 0.86mx60mm taper 75mm
xviii. 2pcs 0.71mx58mm taper 70mm
xix. 4pcs 0.674mx88mm taper 88mm & taper 325mm
xx. 2pcs 0.57mx56mm taper 65mm
xxi. 2pcs 0.44mx54mm taper 60mm
xxii. 4pcs 0.398mx86mm taper 86 & taper 240mm
xxiii. 2pcs 0.32mx52mm taper 60mm
xxiv. 2pcs 0.2mx50mm taper 55mm
xxv. 2pcs 0.09mx48mm NO TAPER

d. Fuselage Reinforcement 90 (4 plies total) Use templates
    i. Mark Kink in Centers
    ii. Two plies at 450mm total width
    iii. Two plies at 400mm total width
e. Spar Web +/-45 (144 pieces total) Use Templates
    i. Mark Centers
    ii. Templates 1-6 are front web
        1. Cut 4 of each (24), right side up (+45)
        2. Cut 4 of each (24), Reversed (-45)
    iii. Templates 7-12 are middle web
        1. Cut 4 of each (24), right side up (+45)
        2. Cut 4 of each (24), Reversed (-45)
    iv. Templates 13-18 are rear web
        1. Cut 4 of each (24), right side up (+45)
        2. Cut 4 of each (24), Reversed (-45)
f. Fuselage Reinforcement +/-45 (12 plies total) Use Templates
    i. Mark Centers and Kink
g. Trailing Edge +/-45 (48 pieces total) Use Templates
    i. TE1-TE6
        1. Cut 2 of each (12),right side up (+45)
        2. Cut 2 of each (12), reversed (-45)
    ii. TE13-18
        1. Cut 2 of each (12),right side up (+45)
        2. Cut 2 of each (12), reversed (-45)
h. Trailing Edge Zeros (32 pieces total)
    i. 8pcs 1.8mx6mm

ii. 8pcs 1.8mx4mm
iii. 8pcs 1.2mx6mm
iv. 8pcs 1.2mx4mm

5. Layup Procedure
    a. Leading Edge Zeros
        i. All pieces are aligned with leading edge of mold
        ii. Lay 1.8mx8mm pieces on bottom and top, both sides of centerline
        iii. Lay 1.2mmx8mm pieces on bottom and top extending to wingtip
        iv. Lay 1.8mx6mm pieces on bottom and top, both sides of centerline
        v. Lay 1.2mmx6mm pieces on bottom and top extending to wingtip
    b. First +45 Skin Top Mold
        i. Lay T1-T12 where T1 is at on left hand of mold when standing at trailing edge looking forward to leading edge
        ii. Start with T6-T7 align kink with mold centerline
        iii. Plies should be aligned fore-aft by butting against leading edge of mold
        iv. Rear edge of ply should be ~5mm ahead of trailing edge insert trough
    c. Debulk top mold
    d. First +45 Skin Bottom Mold
        i. Lay B1-12 where B1 is on left hand of mold when standing at trailing edge looking forward to leading edge
        ii. Start with B6-B7 and align kink with mold centerline
        iii. Plies should be aligned fore-aft by butting against leading edge of mold
        iv. Rear edge of ply should be ~5mm ahead of trailing edge insert trough
    e. Debulk bottom mold for 15 minutes
        i. Use extra wide airdraw II bag on top mold
        ii. Use large diameter hose
        iii. Debulk first plies for 30 minutes
    f. Place leading edge foam support on top mold
        i. Place foam in layflat
        ii. Align with front edge of mold
        iii. Tape in place
    g. First -45 Skin Top Mold
        i. Lay T13-T24, T13 will be on right hand of mold when standing at trailing edge looking forward to leading edge
        ii. Align kink with mold centerline
        iii. Set fore-aft by aligning with rear edge of +45
        iv. Front edge of ply should be ~7mm past leading edge

v. Rear edge of ply should be ~5mm ahead of trailing edge insert trough

h. Debulk top mold for 15 minutes
i. First -45 Skin Bottom Mold
    i. Lay B13-24, B13 and T13 will be on right hand of mold when standing at trailing edge looking forward to leading edge
    ii. Align kink with mold centerline
    iii. Set fore-aft by aligning with rear edge of +45
    iv. Front edge of ply should be ~5mm back from leading edge
    v. Rear edge of ply should be ~5mm ahead of trailing edge insert trough
j. Debulk bottom mold for 15 minutes
k. Spar Cap Top Mold
    i. Lay 6m cap first
    ii. Align center marking with mold centerline
    iii. Align fore-aft, by setting center of spar 135mm aft of leading edge at wing mid-point and 73.4mm aft of leading edge at 3m out from mid-point (90mm and 28.4mm respectively from front edge of spar)
    iv. Lay remaining spar caps, debulking after every 3 plies
l. Spar Cap Bottom Mold
    i. Lay 6m cap first
    ii. Align center marking with mold centerline
    iii. Align fore-aft, by setting center of spar 135mm aft of leading edge at wing mid-point and 73.4mm aft of leading edge at 3m out from mid-point (90mm and 28.4mm respectively from front edge of spar)
    iv. Lay remaining spar caps, debulking after every 3 plies
m. Second -45 Skin Top Mold
    i. Lay T25-T36 where T25 is at on right hand of mold when standing at trailing edge looking forward to leading edge
    ii. Start with T31-T32 align kink with mold centerline
    iii. Front edge of ply should be 12mm ahead of leading edge
    iv. Rear edge of ply should be ~23mm ahead of trailing edge insert trough at wing mid-point, 17mm at dihedral,14mm at 3m out
n. Debulk top mold for 15 minutes
o. Second -45 Skin Bottom Mold
    i. Lay B25-TB36 where B25 is at on right hand of mold when standing at trailing edge looking forward to leading edge
    ii. Start with B31-B32 align kink with mold centerline
    iii. Front edge of ply should be 10mm aft of leading edge
    iv. Rear edge of ply should be ~10mm ahead of trailing edge insert trough at wing mid-point, 9mm at dihedral and 7mm at 3m out

p. Debulk bottom mold for 15 minutes
q. Second +45 skin top mold
    i. Lay T37-T48 where T37 is at on left hand of mold when standing at trailing edge looking forward to leading edge
    ii. Start with T43-T44 align kink with mold centerline
    iii. Front edge of ply should be 17mm ahead of leading edge
    iv. Rear edge of ply should be ~23mm ahead of trailing edge insert trough at wing mid-point, 17mm at dihedral,14mm at 3m out
r. Debulk top mold for 15 minutes
s. Second +45 Skin Bottom Mold
    i. Lay B37-B48 where B37 is at on left hand of mold when standing at trailing edge looking forward to leading edge
    ii. Start with B43-B44 align kink with mold centerline
    iii. Front edge of ply should be 15mm aft of leading edge
    iv. Rear edge of ply should be ~10mm ahead of trailing edge insert trough at wing mid-point, 9mm at dihedral and 7mm at 3m out
t. Debulk bottom mold for 15 minutes
u. Prepare Styrofoam Webs
    i. Cut layflats (Extend 750mm past each end of mold)
    ii. Front and middle webs require 4.5” layflat, rear web 3”
    iii. Put string thorough layflats
    iv. Put foam into layflats
    v. Seal and vacuum layflats
    vi. Bunch excess bag at recess in base of foam
    vii. Tape excess bag at base of layflat and feed in string loop
v. Place Styrofoam webs on top mold
    i. Use templates to position foam
    ii. Debulk to stick styrofoam down to skin
w. Spray adhesive onto 1” peel ply and place peel ply on top of foam webs
x. First +45 Web Ply
    i. Lay +45 Web 1-6 on front Styrofoam web (symmetric, total 12 pcs)
    ii. Lay +45 Web 7-12 on middle Styrofoam web (symmetric, total 12 pcs)
    iii. Lay +45 Web 13-18 on rear Styrofoam web (symmetric, total 12 pcs)
    iv. Align by center marks
y. Debulk Top Mold for 15 minutes
z. First -45 Web Ply
    i. Lay -45 Web 1-6 Reversed on front Styrofoam web (symmetric, total 12 pcs)

ii. Lay -45 Web 7-12 Reversed on middle Styrofoam web (symmetric, total 12 pcs)
iii. Lay -45 Web 13-18 Reversed on rear Styrofoam web (symmetric, total 12 pcs)
iv. Align by center marks

aa. Second -45 Web Ply
i. Lay -45 Web 1-6 Reversed on front Styrofoam web (symmetric, total 12 pcs)
ii. Lay -45 Web 7-12 Reversed on middle Styrofoam web (symmetric, total 12 pcs)
iii. Lay -45 Web 13-18 Reversed on rear Styrofoam web (symmetric, total 12 pcs)
iv. Align by center marks

bb. Second +45 Web Ply
i. Lay +45 Web 1-6 on front Styrofoam web (symmetric, total 12 pcs)
ii. Lay +45 Web 7-12 on middle Styrofoam web (symmetric, total 12 pcs)
iii. Lay +45 Web 13-18 on rear Styrofoam web (symmetric, total 12 pcs)
iv. Align by center marks

cc. Place Vacuum bag at trailing edge insert
i. Place vacuum bag at trailing edge
ii. Fold edge over at joint to ease later removal
iii. Align bag 15mm from trailing edge trough at wing mid-point , 12mm at dihedral and 9mm at wing tip

dd. First Trailing Edge-45 ply
i. Lay -45 TE1-6 Reversed (symmetric, total 12pcs)
ii. Align with first skin +45 ply at trailing edge
iii. Should sit 5mm from trailing edge trough

ee. first Trailing Edge +45 Ply
i. Lay +45 TE1-6 (symmetric, total 12pcs)
ii. Align with first skin +45 ply at trailing edge
iii. Should sit 5mm from trailing edge trough

ff. Place mold inserts
i. Position mold inserts in mold insert trough
ii. Mold inserts are labeled L1-L22 and R1-R22
iii. Lay L1-22 on right hand side of mold when standing at trailing edge looking forward to leading edge
iv. Lay R1-22 on left hand side of mold when standing at trailing edge looking forward to leading edge

gg. Fold trailing plies over
hh. Remove Vacuum bag
ii. Debulk for 15 minutes
jj. Second Trailing edge -45 ply
    i. Lay -45 TE13-18 Reversed (symmetric, total 12pcs)
    ii. Align edge 5mm forward of flat on mold insert top surface
    iii. Should be 5mm forward of first trailing -45 ply
kk. Second Trailing edge +45 ply
    i. Lay +45 TE13-18 (symmetric, total 12pcs)
    ii. Align edge 5mm forward of flat on mold insert top surface
    iii. Should be 5mm forward of first trailing +45 ply and aligned with second -45
ll. Trailing Edge Zeros
    i. On bottom of mold insert place as far into joint as possible
    ii. On top of mold insert place 5mm forward of flat (same as second TE +/-45)
    iii. Lay 1.8mx6mm toward center of wing, top and bottom of mold insert (4pcs)
    iv. Lay 1.2mx6mm at wing ends, top and bottom of mold insert (4pcs)
    v. Lay 1.8mx6mm toward center of wing, top and bottom of mold insert (4pcs)
    vi. Lay 1.2mx6mm at wing ends, top and bottom of mold insert (4pcs)
    vii. Lay 1.8mx4mm toward center of wing, top and bottom of mold insert (4pcs)
    viii. Lay 1.2mx4mm at wing ends, top and bottom of mold insert (4pcs)
    ix. Lay 1.8mx4mm toward center of wing, top and bottom of mold insert (4pcs)
    x. Lay 1.2mx4mm at wing ends, top and bottom of mold insert (4pcs)
mm. Prepare remaining cavity lay flats
    i. Front three cavities need 4.5” layflat
    ii. Rear cavity needs 3” layflat
    iii. Insert string through bags
    iv. Insert thermocouples into middle big (mark positions at middle, dihedral, tip)
    v. Fold bags up and tape them, feeding string through tape
nn. Place peel ply in remaining cavities
oo. Place lay flats in cavities
pp. Fold leading edge foam support over and tape in place (let this sit for a long time)

6. Close mold
    a. Place dowel pins in top mold
    b. Lift bottom mold with crane
    c. Place each end on engine stand
    d. Rotate bottom mold
    e. Lift bottom mold above top mold
    f. Push back carbon at leading edge
    g. Slowly lower bottom mold, continually checking and pushing back leading edge
    h. Allow molds to first touch at end with transverse locating dowel
    i. Fully close mold and remove crane
    j. Pull strings to break tape on internal bags while holding bags firmly in place from opposite end
7. Seal mold
    a. Put breather along mold seam on sides
    b. Close sides with vacuum bag
    c. Close end with vacuum bag
    d. Insert multiple small high temp vacuum lines at each end
    e. Insert large 1.25” diameter hose at end closest to pump

Jacob Bruce Patterson was born in Austin, Texas on May 4th, 1989, to Bruce and Laura Patterson. After graduating from McCallum High School in Austin, Tx, he attended Lehigh University in Bethlehem, Pennsylvania. In January of 2012 he completed a Bachelors of Science in Mechanical Engineering with honors. He then continued on at Lehigh to pursue a Master of Science in Mechanical Engineering and plans to continue on to a PhD in Mechanical Engineering at Lehigh.